Catena 258 (2025) 109270

Contents lists available at ScienceDirect

Catena

journal homepage: www.elsevier.com/locate/catena

Comparing recent and buried Chernozems/Phaeozems in Central Germany: Soil transformation and human impact since 3.8 ka

Hans von Suchodoletz[a,b,*], Birgit Schneider[a], Anna Skokan[c], Teresa Nitz[a], Bruno Glaser[d], Steven Polivka[d], Katja Wiedner[d,e], Frank Schlütz[f], Torsten Schunke[g], Peter Kühn[h]

[a] *Institute of Geography, Leipzig University, Leipzig, Germany*
[b] *Institute of Geography, Jena University, Jena, Germany*
[c] *Institute of Geography, TU Dresden, Dresden, Germany*
[d] *Martin-Luther University Halle-Wittenberg, Institute of Agricultural and Nutritional Sciences, Soil Biogeochemistry, Halle/Saale, Germany*
[e] *Present Address: Gütegemeinschaft Kompost Ost e.V, Doberlug-Kirchhain, Germany*
[f] *Institute of Pre- and Protohistoric Archaeology, Kiel University, Kiel, Germany*
[g] *State Office for Monument Preservation and Archaeology of Saxony-Anhalt, Halle/Saale, Germany*
[h] *Chair of Soil Science and Geomorphology, Tübingen University, Tübingen, Germany*

A R T I C L E I N F O

Dataset link: Analytical data of a buried and a recent surficial Chernozem in the Bornhöck area in Central Germany (Original data)

Keywords:
Chernozems/Phaeozems
Central Germany
Soil formation
Human impact
Lignite fly ash
Carbonate dynamics
Soil isotopes

A B S T R A C T

Chernozems and Phaeozems in Central Germany have been subject to both natural alterations and human influences for millennia. This study systematically compares a buried Early Bronze Age Chernozem, preserved under the Bornhöck burial mound, with a neighboring surface soil to analyze soil transformation and human impact over the past 3.8 ka.

Our results indicate that, unlike in more humid Central European regions where former Chernozems/Phaeozems have been entirely transformed into Luvisols, soils in the study area have undergone slower alterations due to the dry regional climate and high carbonate content of the parent material. Key pedogenic processes include gradual decalcification, black carbon decomposition, and weak clay illuviation. Before and during the Early Bronze Age human impact was minimal, limited mainly to shallow plowing (<20 cm) and phosphorus enrichment from human and/or animal excrements. Especially since the industrialisation human impact strongly increased, what is evident in higher values of magnetic susceptibility, the enrichment of heavy metals and sulfur likely due to fly ash deposition from lignite-burning power plants, and shifts in the isotopic composition of soil organic matter from agricultural practices. The most pronounced human impact since that time has been secondary recalcification due to fly ash input, which halted the natural transformation of Chernozems/Phaeozems into Luvisols and modified soil biota conditions. Given ongoing climate change and increasing regional temperatures, decalcification of these secondary carbonates should strongly decelerate or even stop.

1. Introduction

Soils provide important ecosystem functions such as carbon (C) storage, nutrient storage cycling, biomass (food) production, water filtration or a high biodiversity, and they archive the geological and archaeological heritage (Adhikari and Artemink, 2016, Keesstra et al., 2016, Pietsch and Kühn, 2017). Driven by natural factors such as topography, parent material, climate, organisms and time, soil properties constantly change over time (Jenny, 1994). Furthermore, human activities further change soil properties and their development (Dror et al., 2022), what already began during the Neolithic period through agriculture and construction activities. Subsequently, human impact increased with growing population and new economic activities, particularly since the 19th century CE due to industrialization (Henkner et al., 2018, Meharg and Meharg, 2021, Tian and Niu, 2015). To understand the current soil properties and their possible future development between natural and human factors, the formation history of the individual soils should be systematically analysed (Storozum et al., 2020). Ideally, this can be achieved by comparing the properties of buried soils with those of similar neighboring surface soils. During the last decades this approach has repeatedly been realized especially in East-Central and Eastern Europe and Denmark for sites with palaeosols

* Corresponding author at: Institute of Geography, Leipzig University, Leipzig, Germany.
E-mail address: hans.von.suchodoletz@uni-leipzig.de (H. von Suchodoletz).

https://doi.org/10.1016/j.catena.2025.109270
Received 13 May 2025; Received in revised form 19 June 2025; Accepted 27 June 2025
Available online 6 July 2025
0341-8162/© 2025 The Author(s). Published by Elsevier B.V. This is an open access article under the CC BY license (http://creativecommons.org/licenses/by/4.0/).

buried by prehistoric burial mounds (kurgans) (Khokhlova et al., 2007, Breuning-Madsen et al., 2009, Hejcman et al., 2013, Alexandrovskiy et al., 2014, Barczi and Nagy, 2016, Pampura et al., 2019, Hildebrandt-Radke et al., 2019, Kabała et al., 2019, Krupski et al., 2024).

Black-colored humus-rich Chernozems and Phaeozems cover ~420 million ha worldwide (IUSS Working Group WRB, 2022, Chesworth, 2016). As they are among the most fertile soils in the world, they have often been used for agriculture for several millennia (Altermann et al., 2005, Liu et al., 2012, Brigand and Weller, 2013, Lisetskii et al., 2013, Pleasant, 2015, von Suchodoletz et al., 2019). The westernmost continuous Chernozem/Phaeozem region of Eurasia is located in the dry area in the eastern lee of the Harz Mountains in Central Germany (Central German dry area), with annual precipitation of about 440–600 mm/a (Eckmeier et al., 2007, von Suchodoletz et al., 2019; Fig. 1). Unlike in other Central European regions with anthropogenic Chernozems/Phaeozems (Gerlach et al., 2012, Leopold et al., 2011, Acksel et al., 2017, Kasielke et al., 2019), their natural formation is attributable to the high carbonate contents of their parent materials such as aeolian and fluvial sediments, and the dry subcontinental climate already during the early Holocene (Lorz and Saile, 2011, von Suchodoletz et al., 2019). These factors may have favored suitable living conditions for anecic earthworms (Dreibrodt et al., 2022). Similar with Chernozems/Phaeozems in central Hesse, the eastern Czech Republic or southern Poland, their formation started prior to regional Neolithic settlement and lasted until the late Middle Holocene when the regional climate became more humid (Hejcman et al., 2013, Kühn et al., 2017, Kabała et al., 2019, von Suchodoletz et al., 2023). In Central Germany these soils were degraded to varying degrees by decalcification, followed by silicate weathering, clay translocation and clay formation since that time (Baumann et al., 1983, Eckmeier et al., 2007, von Suchodoletz et al., 2019), whereas in other regions they were completely converted to other soil types such as Luvisols and Retisols (Hejcman et al., 2013, Kabała et al., 2019). In contrast, the development of younger Chernozems/Phaeozems at some archaeological sites in the eastern Harz foreland (Dreibrodt et al., 2023) may be linked with the surfacing of carbonate-rich parent material by human activity.

Some of the highly fertile Central German Chernozems/Phaeozems (Liedtke and Marschner, 2003), agriculturally used for several millennia (Bruckmeier and Grund, 1994, von Suchodoletz et al., 2019), are located in the Central German industrial region. Here, intensive industrialization with large-scale lignite burning as the main energy source started since the end of the 19th century CE (Neumeister et al., 1991). The millennia-long human activities strongly impacted regional soils by e.g. soil erosion and fertilization with natural fertilizers, followed by the application of industrial fertilizers and pesticides as well as atmospheric pollutants since the industrialisation (Neumeister et al., 1991, Bruckmeier and Grund, 1994, Manz et al., 2001, Koch et al., 2002, Dreibrodt et al., 2013). Several studies investigated human impact on soils in Central Germany since the 19th century CE so far (Neumeister et al., 1991, Manz et al., 2001, Koch et al., 2002, Dultz and Kühn 2005, Rinklebe et al., 2019). However, apart from one study where a Late Neolithic buried Chernozem was compared with the neighboring surficial soil using a limited number of laboratory analyses (Baumann et al., 1983), the millennia-long natural and human alterations of the Central

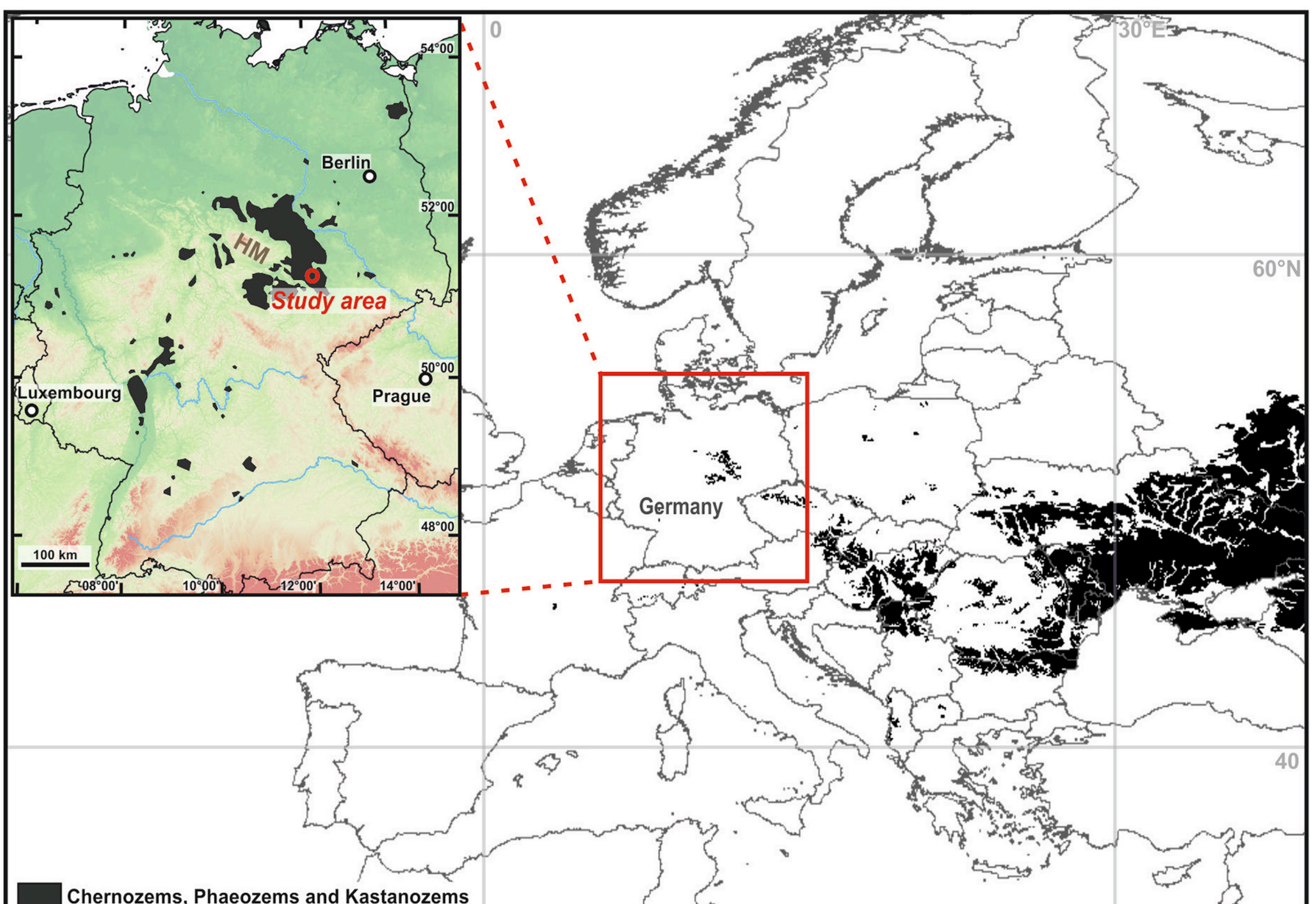

Fig. 1. Distribution of soils with mollic epipedon in Europe: Chernozems, Phaeozems, Kastanozems (black coloring; taken from FAO/IIASA/ISRIC/ISSCAS/JRC 2012: Harmonized World Soil Database (v. 1.2). FAO Rome, Italy and IIASA, Laxenburg, Austria). Inset: The study area in the Chernozem/Phaeozem area of Central Germany (red circle). The distribution of Chernozems/Phaeozems is shown in black (after Eckmeier et al., 2007, modified), and the Central German industrial region in yellow (after LMBV, 2011, 2019). HM = Harz Mountains.

German Chernozems/Phaeozems were not systematically studied so far using a systematic comparison of recent and buried soils.

To fill this gap we analysed the changes of a fertile Chernozem in the Central German industrial region, located on the western edge of the Eurasian Chernozem/Phaeozem area (Fig. 1), within the last 3800 years. For this purpose, we exemplarily compared the properties of a Chernozem buried by the Early Bronze Age Bornhöck burial mound (Meller & Schunke, 2016) with those of a similar neighboring surficial soil, by using field-based soil description, pedological, sedimentological and isotope analyses as well as micromorphological investigations. These analyses should allow to recognize systematic differences between the buried and the recent soil developed on similar parent material.

2. Study area and study site

The study area is located in the Leipzig Basin that is filled with Paleogene to Quaternary loose sediments (SLUG, 1992, Wagenbreth & Steiner, 1989). During the Quaternary, this lowland was repeatedly covered by ice shields of the Elsterian and Saalian glaciations, followed by (sand) loess deposition and periglacial reworking during the latest Saalian and Weichselian cold periods (Eissmann, 2002). The region shows a fully humid warm temperate Cf-climate with maximal summer precipitation (Kottek et al., 2006). Mean annual temperature is around 9.1 °C, and due to its location at the margin of the Central German dry area mean annual precipitation is around 551 mm (www.dwd.de). The early Holocene climate was warmer and drier and more subcontinental compared with today, followed by more humid conditions since ca. 6.7 ka and especially since 5.8 ka (Wennrich et al., 2005). The potential natural vegetation is *Quercus-Carpinus* forests with only few proportions of *Fagus* (Bohn & Welß, 2003), and for the Early/Middle Holocene *pinus* forests with interspersed non-forested habitats as regional natural pre-Neolithic vegetation are suggested (Litt, 1992, von Suchodoletz et al., 2024, Tinapp et al., 2025). However, the region is intensively used for agriculture and hence largely forest-free today, and agricultural land use started ca. 7.5 ka during the early Neolithic. Subsequently, the region was nearly continuously inhabited with varying intensities (Tinapp & Stäuble, 2000). The study area is situated in the south-eastern part of the Central German Chernozem/Phaeozem region (Fig. 1 inset) (LGBSA, 1995, SLULG, 1993), where Chernozems and Phaeozems are spatially closely interfingered with each other (Eckmeier et al., 2007), as well as in the Central German industrial region that was strongly industrialized since the 19th century CE.

The study site is located on a flat Saalian moraine plateau about 2 km north of the valley of the Weiße Elster River at about 110 m a.s.l. (Fig. 2). In this area, Chernozems/Phaeozems had developed mainly in a 40–70 cm thick layer of sandy loess (Lehmkuhl et al., 2021) originating from the last phase of the Pleistocene. The sandy loess layer is separated by a stone layer from the underlying Saalian glacial moraine deposited >130 ka ago (Neumeister, 1971, Eissmann, 2002). The burial mound Bornhöck was erected during the Early Bronze Age ca. 3.8 ka ago, with a diameter of ca. 65 m and a height of 12–13 m. During the Middle Ages and Early Modern Age the burial mound grew to almost 90 m in diameter and 15 m height (Schunke, 2018). During the second half of the 19th century CE it was largely destroyed (Meller & Schunke, 2016). However, the original Chernozem buried below the Bornhöck burial mound remained protected against subsequent agricultural activity and atmospheric processes by a cover of several decimeters of archaeosediments until today.

3. Methods

3.1. Fieldwork

The buried Chernozem profile below the Bornhöck (BH-II) with a

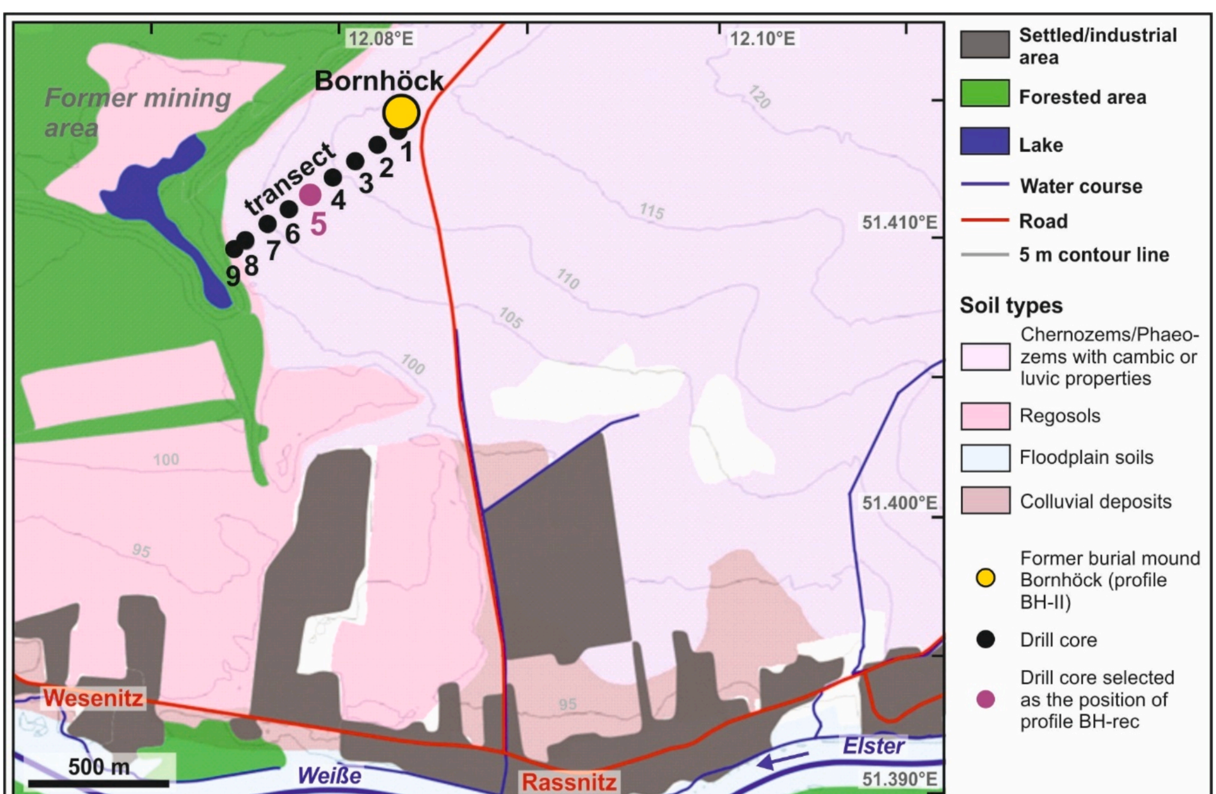

Fig. 2. Soil map of the study area. Numbers indicate coring locations of the catena, with core 5 located nearby studied recent profile BH-rec highlighted in violet (topography: DEM2 ©GeoBasis-DE/LVermGeo LSA; water courses: ©Bundesanstalt für Gewässerkunde (BfG) 2023; roads, forested and settlement areas: ©GeoBasis-DE/BKG 2022, soils: Landesamt für Geologie und Bergwesen Sachsen-Anhalt – LAGB: Preliminary soil map 1: 50.000).

depth of 80 cm was studied during ongoing excavations by the State Office for the Preservation of Archaeology Saxony-Anhalt in July 2018. This profile was located slightly to the north below the center of the former burial mound, and remained buried by a residual cover of several decimetres of archaeosediments even after the extensive destruction of the burial mound in the second half of the 19th century CE. Mostly bioturbation features but no anthropogenic remains were found during former micromorphological investigations of this buried soil. Together with downwards systematically increasing bioturbation-related luminescence ages going back to the Pleistocene/Holocene transition (von Suchodoletz et al., 2023), this argues for a natural Chernozem whereas an Anthrosol can most likely be excluded.

Starting approximately 60 m south of the center of the former Bornhöck burial mound and going towards the South-West, we investigated a 750 m long catena that consisted of 9 drill cores with depths of 1 m using an Atlas Copco Cobra Pro hammer with a 60 mm-diameter open corer (Fig. 2). The catena began on the flat Saalian plateau and ended in a small tributary dry valley of the Weiße Elster River, encompassing about 12 m altitudinal difference (Fig. 3). A comparison of the core stratigraphies showed that core 5, which was located about 400 m south-west of buried profile BH-II, had the best visible preservation of the soil horizons and is thus the best representative profile of the Chernozems/Phaeozems occurring in the Bornhöck area today. Therefore, a 110 cm deep soil profile (BH-rec) was dug here in summer 2019.

The description of the soil profiles and the cores of the catena mainly followed the WRB (IUSS Working Group WRB, 2022), however, to also account for soil genesis, we did not always follow the WRB rules of minimum thicknesses of soil horizons.

3.2. Pedological and sedimentological analyses

For these analyses sieved sample material < 2 mm was used.

Grain size analyses were performed using 10 g of bulk sample material. After destroying carbonate with 10 and 32 % HCl and organic matter with 35 % H_2O_2, the samples were dispersed in 10 ml 0.4 N sodium pyrophosphate solution ($Na_4P_2O_7$) followed by ultrasonic treatment for 45 min. Sand contents (63–2000 μm) were determined by wet sieving. The material < 63 μm was measured with X-ray granulometry (XRG) using a SediGraph III 5120 (Micromeritics).

Carbonate contents were measured according to Scheibler in an Eijkelkamp Calcimeter apparatus, i.e., based on the CO_2-volume produced during the reaction of the sediments with 10 % HCl.

pH-values were measured using a pH-meter 196 (WTW) after 2 h of soaking.

To determine *element contents* using a Spectro Xepos X-ray fluorescence spectrometer, air dried sample material was ground in a vibration mill for 10 min to obtain the required grain size <30 μm and for homogenisation. Prior to measurement, a 32 mm-pellet was produced by mixing and pressing 8 g of the ground material with 2 g CEREOX Licowax. A large part of the carbonate in regional Pleistocene sediments originates from Triassic sediments of the Thuringian Basin (Neumeister, 1971), containing significant amounts of dolomite (Schwahn & Garmann, 1976). Hence, given the robustness of this proxy against the occurrence of dolomite, we applied the Chemical Proxy of Alteration (CPA) as a proxy of chemical silicate weathering (Buggle et al., 2011):

$$CPA = 100 * Al_2O_3/(Al_2O_3 + Na_2O) \text{ (in molar proportions)} \quad (1)$$

Mass-specific magnetic susceptibility was measured using a Bartington MS3 magnetic susceptibility meter equipped with a MS2B dual frequency sensor. After softly grounding and densely packing the material into plastic boxes, volumetric magnetic susceptibility was measured with a frequency of 0.465 kHz and normalized with the sample mass.

Total organic carbon (TOC) was determined by measuring C_{total} of the milled material <30 μm with a Vario EL cube elemental analyser, and subsequently subtracting inorganic carbon (taken from carbonate measurements) from C_{total}.

Proportion and composition of *black carbon (BC)* were determined by measuring benzene polycarboxylic acids (BPCA) contents and patterns according to Glaser et al. (1998), modified by Brodowski et al. (2005). This method comprises polyvalent cation removal with 4 M trifluoroacetic acid (Brodowski et al., 2005) followed by nitric acid digestion (170 °C, 8 h under pressure), cation exchange chromatography, trimethylsilylation (derivatization) and gas chromatography with flame ionization detection (Glaser et al., 1998). The sum of individual BPCA

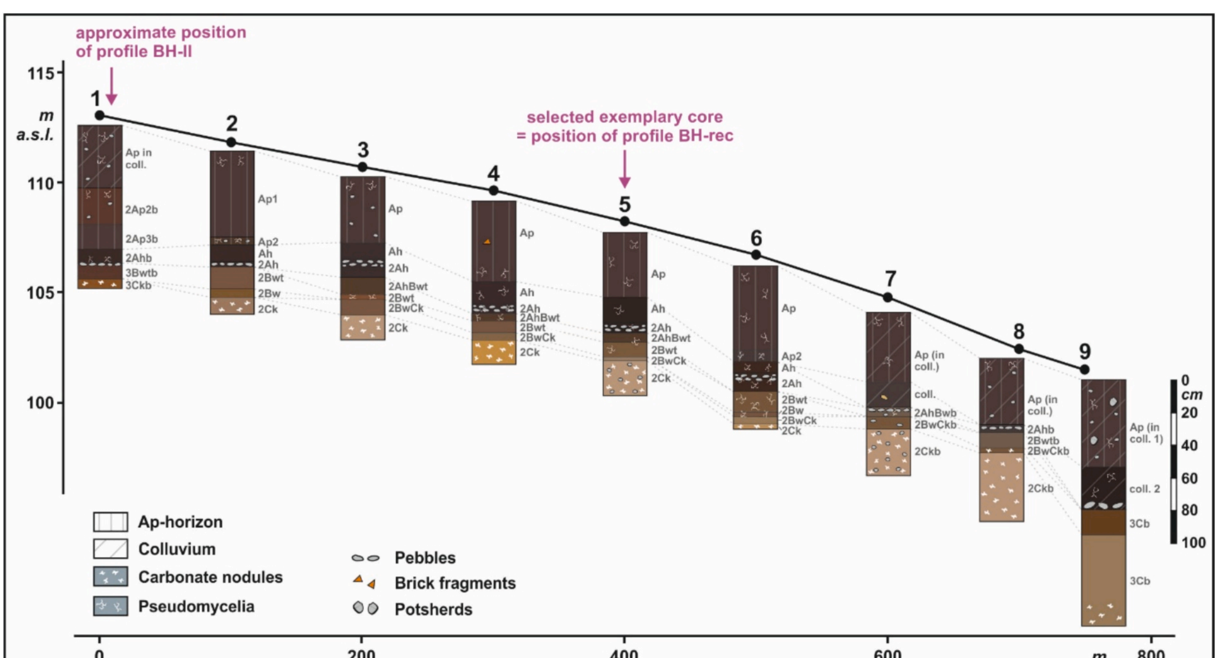

Fig. 3. Catena, southwest of the former Bornhöck burial mound (location see Fig. 2). Detailed descriptions of the cores are given in Table S1. Given that core 5 had the best visible preservation of the soil horizons and is thus the best representative profile of the current Chernozems/Phaeozems in the Bornhöck area, its position was selected to dig profile BH-rec that was studied in more detail (Fig. 4).

was converted to the BC content by multiplication with 2.27 (conversion factor for charcoal; Glaser et al., 1998).

Lignin phenols were extracted from 100−500 mg of dried soil material using the cupric oxidation (CuO) method of Hedges and Ertel (1982) modified by Goñi and Hedges (1992): The samples were transferred into Teflon digestion tubes together with 100 mg of $(NH_4)_2 Fe(SO_4)_2 * 6 H_2O$, 500 mg of CuO, 50 mg of glucose, 1 ml of ethylvanillin solution (100 mg/l) as internal standard 1, and 15 ml of 2 M NaOH, and digested at 170 °C for 2 h under elevated pressure. The reaction products were cooled overnight and transferred into centrifuge tubes. Then the phenolic compounds were purified by adsorption on C_{18} columns, desorbed by ethylacetate and concentrated under a stream of nitrogen gas for 30 min. The residue was dissolved in 1 ml phenylacetic acid (PAA) as internal standard 2 to determine the recovery of ethylvanillin before derivatization (Amelung et al., 2002, Möller et al., 2002). Finally, the samples were derivatized using 200 µl of BSTFA and 100 µl of pyridine. The oxidation products of phenolic compounds were quantified using a gas chromatograph coupled to a mass Spectrometer (SHIMADZU, GC–MS–QP2010, Kyoto, Japan). For vegetation reconstruction we used the ratios S/V (syringyl-to vanillyl units) and C/V (cinnamyl-to vanillyl units) (Thevenot et al., 2010).

3.3. Isotope analyses

The samples were pulverized in a vibratory mill (10 min, <30 µm). The $\delta^{15}N$ was measured directly, and the $\delta^{13}C$ after carbonate removal as described by Pötter et al. (2021), involving treatment with 5 % HCl in a water bath (50 °C/4h) followed by two washes and subsequent drying overnight at 50 °C. Per isotope measurement, three subsamples each about 45 mg were weighed into tin capsules. The isotope composition was determined at the stable isotope laboratory IsoLab Schweitenkirchen (Germany) on a CF-IRMS device utilizing internal standards, reporting the results in δ-notation as ‰ (^{13}C vs. V-PDB, ^{15}N vs. air).

3.4. Micromorphology

For micromorphological investigation, three undisturbed and oriented soil samples were taken from profile BH-recent, and two samples from buried profile BH-II (sample positions see Fig. 4, the latter formerly described in von Suchodoletz et al., 2023). After air-drying and impregnating with Oldopal P 80–21, hardened blocks were cut and sliced into 90 * 60 mm thin sections and scanned with a flatbed scanner. The thin sections were described at 50–400 magnification under a polarizing light microscope, mainly using the terminology of Stoops (2021).

4. Results

4.1. Catena

The upper parts of cores 1, 7, 8 and 9 show colluvial deposits with thicknesses between 38 and 80 cm (Fig. 3). Core 1 was located on top of the Saalian moraine plateau near the Bornhöck burial mound (Fig. 2). The colluvial deposit is younger than the Bornhöck burial mound since it is underlain by several buried Apb horizons whereof the upper one has a thickness >20 cm, i.e. thicker than Bronze Age plough horizons (Pavelka et al., 2017, Scherer et al., 2021). Cores 7–9 with colluvial deposits were located at the footslope in the southwestern part of the catena. The stone

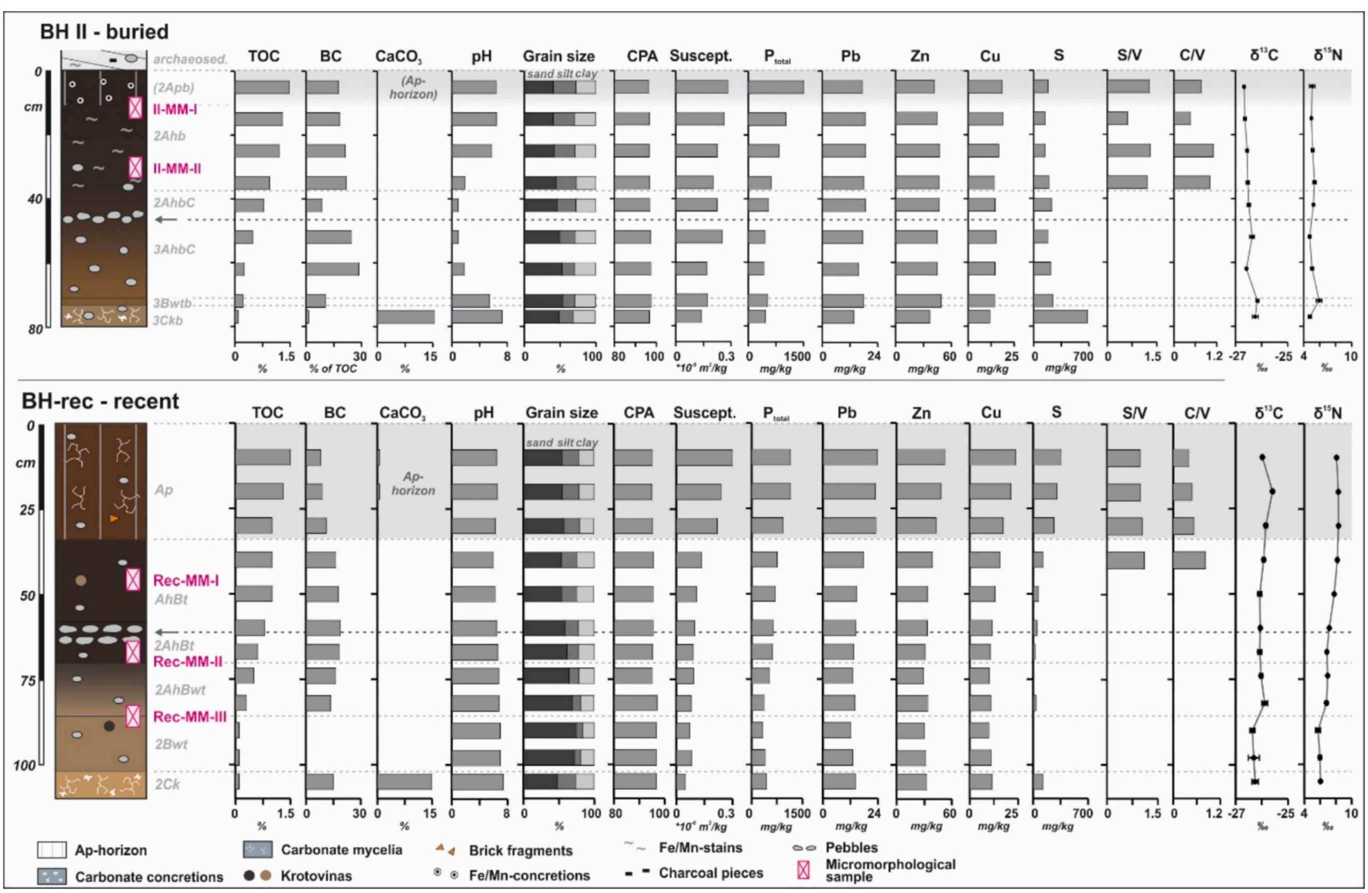

Fig. 4. The studied profiles with analytical values and positions of the micromorphological samples. *[TOC = total organic carbon, BC = black carbon, $CaCO_3$ = calcium carbonate, pH = pH-value, CPA = Chemical Proxy of Alteration; Suscept. = mass-specific magnetic susceptibility, P_{total} = total phosphorous, Pb = lead, Zn = zinc, Cu = copper, S = sulphur, S/V = ratio of syringyl-to vanillyl units, C/V = ratio of cinnamyl-to vanillyl units].*

line (pebbles), separating the lower Saalian moraine from the overlying sandy loess, was found at depths between 85 and 40 cm in cores 1–8. In contrast, in core 9 a colluvial clast layer was observed at the base of the colluvial deposits. Unlike the other cores, due to soil erosion cores 7, 8 and 9 only showed very thin or no sandy loess layers.

All cores showed dark-colored Ap horizons reaching down between 38 and 53 cm depth. The deeper Ap horizons must partly be composed of locally relocated colluvial material filling former small-scale topographic depressions, since their depth exceeded the typical depth of current Ap horizons of about 30 cm (Schatz 2023). Darker-coloured Ah/Ahb horizons are found below the Ap horizons with the exception of cores 7 and 9, where colluvial layers occur. Characteristically AhBwt horizons were found below the Ah/Ahb horizons, followed by Bwt, Bw and/or BwCk and Ck horizons. The colluvial deposit in core 7 covers an AhBwb horizon, followed by the BwCkb and downwards the Ck-horizon. All Ck horizons at the core bases showed intensive secondary carbonate precipitations. Furthermore, apart from some completely decalcified horizons in cores 7 and 8 the upper horizons in the catena showed pseudomycelia or some carbonate in their matrices.

The detailed field stratigraphies of the cores can be found in Table S1.

4.2. Buried profile BH-II

The buried Chernozem is covered by about 70–80 cm of stratified black-coloured archaeosediments of the former burial mound Bornhöck (Fig. 4). Earlier micromorphological investigations of this buried Chernozem showed mainly bioturbation features, but no human remains. Together with systematically downward increasing bioturbation-related luminescence ages dating back to the Pleistocene/Holocene transition (von Suchodoletz et al., 2023) this indicates a natural Chernozem without significant human influence. The luminescence properties of a sample taken from the 2Ahb horizon in a depth of about 10 cm indicate strong sediment bleaching by ploughing until about 3.8 ka, so the uppermost 10–20 cm represent a 2Apb horizon (von Suchodoletz et al., 2023). Fe nodules up to 4 mm thick are often found in the uppermost 10 cm, whereas Fe precipitations occur along root channels in the lower part (Fig. 4). This reflects stagnating water at the boundary between the overlying archaeosediments and the paleosol. The soil color changes from black (10YR2/1) to very dark brown (10YR2/2) at 28 cm, where single brownish Fe-oxide stains and occasional pebbles occur. The dark colors qualify this horizon as "chernic", being characteristic for Chernozems (IUSS Working Group WRB, 2022). In the 2AhbC/3AhbC horizon the color is dark yellowish brown (10YR4/4) in the lower part, and small black clay coatings occur in macropores, which, however, could not be verified micromorphologically. The stone layer, separating the sandy loess from the underlying Saalian moraine, is at ca. 45 cm. Above the stone layer only a few pebbles are found and the texture is clay loam, whereas the pebble amount increases below the stone layer and the texture changes to sandy clay loam. The 3Btwb horizon is dark yellowish brown (10YR 4/4). Whereas the basal yellowish brown (10YR 5/4) 3Ckb horizon is strongly calcareous including carbonate nodules, the soil material above 73 cm was non calcareous in the field. The detailed field stratigraphy of profile BH-II can be found in Table S2a.

The Apb horizon is characterized by the highest TOC values of 1.5 %, and downwards the values systematically decrease. In contrast, the proportion of Black Barbon (BC) of TOC slightly increases downwards to reach its maximum of about 22 % in the 2Apb/2Ahb horizon, and below the values strongly drop. A very low carbonate content of about 0.1 % was analytically found in the 2Apb horizon. The underlying horizons are carbonate-free, whereas the maximum of 15.4 % carbonate is found in the Ck horizon. pH values of 7.2 in the upper part of the profile strongly decrease downwards to values <5 in the central part, and strongly increase to their maximum of 7.6 in the 3Ck horizon. In the sandy loess layer sand slightly increases downwards to 46 % and silt slightly decreases from 32 to 26 %. In the Saalian moraine sand and silt show irregularly varying proportions and a slight increase of clay, with maximal sand contents of 54 %. The Chemical Proxy of Alteration (CPA) shows largely similar values between 96.5 and 97.5 throughout the profile, with slightly higher values in the 3AhbC horizon. Mass-specific magnetic susceptibility shows the highest value of $0.28*10^{-6}$ m^3/kg in the 2Apb horizon, and slightly decreases downwards with a slight intermediate increase in the upper 3AhbC horizon. Total phosphorous (P_{total}) shows its highest value of 1500 mg/kg in the 2Apb horizon, and downwards the values systematically decrease. Lead (Pb), zinc (Zn) and sulphur (S) do not show any enrichment in the upper part of the profile, whereas copper (Cu) shows slightly enriched values of 18.9 and 16.7 mg/kg in the 2Apb and upper 2Ahb horizon. The ratios S/V and C/V show high values of 1.3 and 0.8 in the 2Apb horizon, strongly drop in the uppermost 2Ahb horizon, and increase again in the lower 2Ahb horizon to values of 1.3 and 1.1, respectively. The $\delta^{13}C$ values vary between −26.2 and −26.7 ‰ showing a slight increasing trend downwards, and $\delta^{15}N$ irregularly varies between 4.8 and 5.9 ‰ throughout the profile. The analytical values can be found in von Suchodoletz et al. (in press).

Both thin sections II-MM-I and II-MM-II show a large number of passage features mainly produced by earthworms, snails and mollusks, consisting of discontinuously distributed and often compacted crumbs (Fig. 5a, b). Their large number indicates intense and nearly complete soil mixing due to bioturbation by mesofauna. The high porosity is generally made up of (mamillated) vughs and channels, and partly accommodating planes in sample II-MM-I indicate a weakly developed subangular blocky microstructure. No clay coatings indicating clay relocation were found in both samples. For further information about the micromorphology of profile BH-II please see von Suchodoletz et al. (2023).

4.3. Recent profile BH-rec

The upper part down to 34 cm is taken by the dark brown-coloured (10YR3/3) Ap horizon (Fig. 4). Down to 70 cm follows the very dark brown (10YR2/2) AhBt/2AhBt horizon, containing initial clay coatings and visible passage features in its upper part. In a depth of 40 cm a light-colored crotovina is found, and between ca. 55 and 60 cm the stone layer, separating the upper sandy loess from the underlying Saalian moraine, is developed. Accordingly, above the stone layer only singular pebbles are found, and the material exclusively consists of sandy clay loam. In contrast, below the stone line the pebble amount increases and the texture varies between sandy clay loam and sandy loam. Down to 86 cm follows the 2AhBwt horizon, where the color changes downwards to yellowish brown (10YR5/4). Between 86 and 102 cm follows the yellowish brown 2Bwt horizon, where some dark-coloured material was washed in downwards and visible brownish clay coatings are found especially in passage features. Here, a dark-colored crotovina was found in a depth of 90 cm. At the base of the profile a brownish yellow (10YR6/6) 2Ck horizon follows down to 110 cm. All horizons were found to be carbonatic in the field and pseudomycelia occur in the Ap horizon, and the 2Ck horizon is strongly carbonatic and contains carbonate nodules. The dark color of the AhBt/2AhBt horizon qualifies it as 'chernic', and together with initial clay coatings and the existence of carbonate especially in the upper part of the profile we classified this soil as a calcic Chernozem with luvic properties [German: Parabraunerde-Kalkschwarzerde] (IUSS Working Group WRB, 2022, Altermann et al., 2005). The detailed field stratigraphy of profile BH-rec can be found in Table S2b.

The highest values of total organic carbon (TOC) of up to 1.5 % are found in the Ap horizon. The TOC values show a first drop in the AhBt horizon, and a second drop from the 2AhBt horizon downwards. In contrast, the proportion of black carbon (BC) of TOC increases downwards to reach the highest value of 18.9 % at the transition between the AhBt and 2AhBt horizon, before the values drop again. Low carbonate contents between 0.6 and 0.2 % are found in the Ap horizon. The underlying horizons are largely free of carbonate, before the values reach

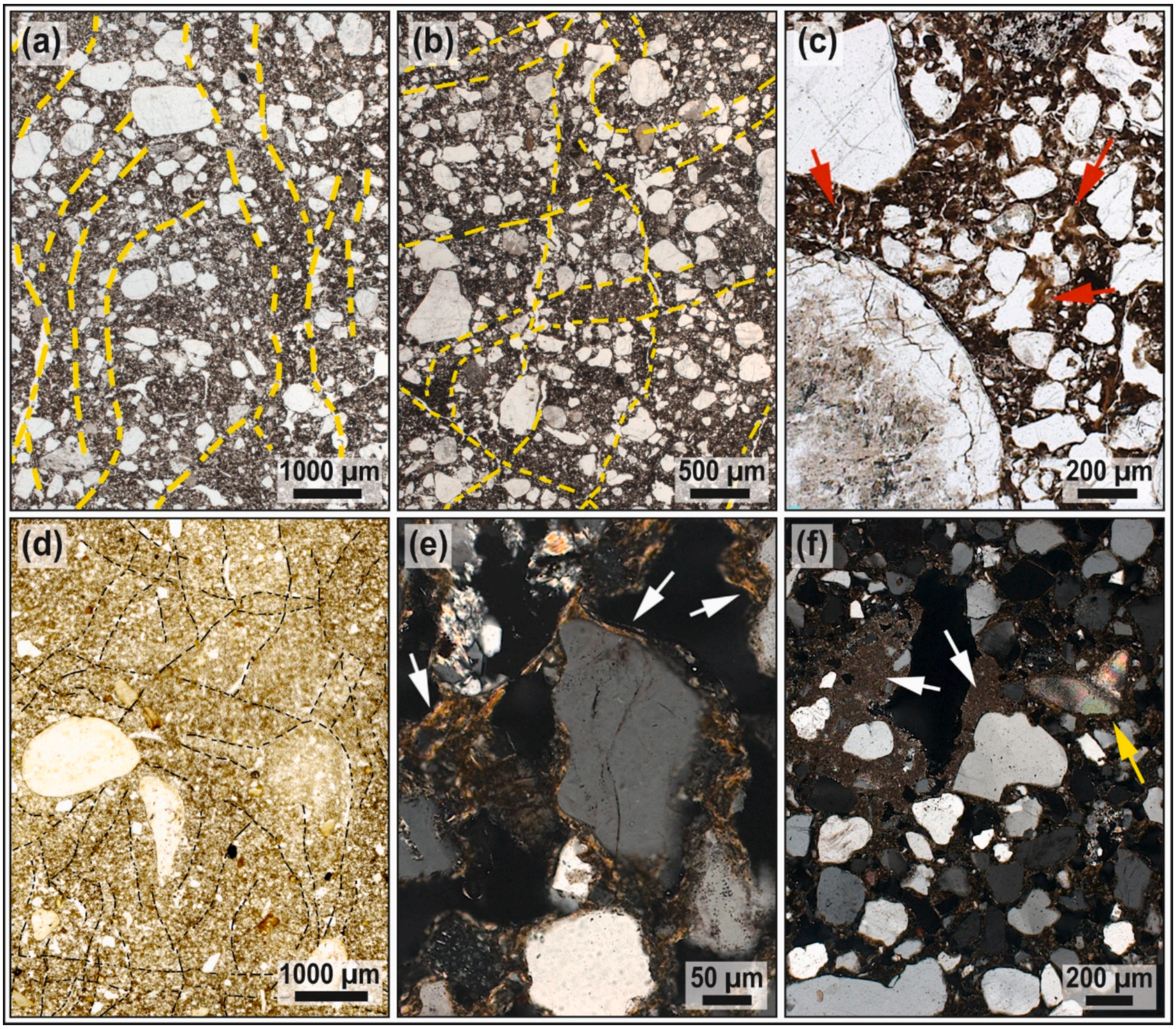

Fig. 5. (a) II-MM-I: Dashed lines indicate complete infillings of passage features caused by soil mesofauna – plane polarized light; (b) II-MM-II: Dashed lines indicate complete infillings of passage features caused by soil mesofauna, note that different generations of passage features cross each other – plane polarized light; (c) Rec-MM-I: Few dark brown clay coatings (red arrows) with maximum thickness of 50 μm – plane polarized light; (d) Rec-MM-II: Soil horizon completely reworked by soil mesofauna (dashed lines indicate passage features) – scan of thin section 6 × 9 cm; (e) Rec-MM-III: White arrows point at weakly developed yellow brown clay coatings, black areas are voids, note the chito-gefuric related distribution of the fine mass – crossed polarized light; (f) Rec-MM-III: Thick (<200 μm) micritic hypocoating to coating (white arrows), shell fragment (yellow arrow) – crossed polarized light.

their maximum of 14.9 % in the 2Ck horizon. The total profile shows basic pH values > 7, with the highest value of 7.7 found in the 2Ck horizon. The sandy loess layer shows a slowly downwards rising sand content up to 59 % and also clay slightly increases, whereas silt slightly decreases. In the Saalian moraine sand content strongly increases downwards to values of about 75 %, and drops to 48 % in the 2Ck horizon. In parallel silt and clay slightly decrease downwards to values of 9 and 18 %, respectively, before increasing in the Ck horizon. The Chemical Proxy of Alteration (CPA) shows largely similar values between 95 and 97 throughout the profile, with slightly higher values in the lower part. Mass-specific magnetic susceptibility, total phosphorous (P_{total}), lead (Pb), zinc (Zn), copper (Cu) and sulphur (S) all show elevated values in the Ap horizon, and their contents systematically decrease downwards. The ratio S/V slightly increases downwards from the Ap to the AhBt horizon to a value of 1.1, and the ratio C/V slightly increases throughout the Ap horizon before showing a sudden increase to 0.8 in the AhBt horizon. δ^{13}C varies between −25.6 and −26.4 ‰ with a downwards decreasing trend throughout the profile. δ^{15}N varies between 5.7 and 8.3 ‰, showing the highest values in the Ap horizon. The analytical values can be found in von Suchodoletz et al. (in press).

In all three micromorphological samples, complete reworking by the soil mesofauna, such as earthworms, snails and molluscs, was observed. The related passage features consist of crumbly complete to incomplete infillings which are mostly continuously distributed (Fig. 5d). A channel microstructure is characteristic for all three samples, and additionally samples Rec-MM-II and Rec-MM-III show a weakly developed crumbly microstructure. In samples Rec-MM-I (Fig. 5c) and Rec-MM-III (Fig. 5e) very small brown limpid and speckled brown clay coatings are found (<30 μm in thickness). Micritic hypocoatings to coatings with crystallitic b-fabric occur in and around some channels in Rec-MM-III (Fig. 5f).

5. Discussion

5.1. Alteration of the regional Chernozems/Phaeozems during the last 3.8 ka

Advancing pedogenesis changes kind and thickness of soil horizons, and in case of carbonate-containing parent material also lowers the decalcification depth (Schalich, 1988). Hence, we compared soil horizon thicknesses and decalcification depths between both studied profiles:

With 102 cm, the total soil thickness in recent profile BH-rec is larger compared with 73 cm in buried profile BH-II (Fig. 4). This difference concerns both the humus-rich upper horizons (A, AB) with total thicknesses of 86 and 70 cm, and the (largely) decalcified non-humic lower soil horizons (B) showing thicknesses of 16 and 3 cm. On the one hand, this difference could be caused by geologic factors: The sand content in BH-rec is generally about 10–20 % higher compared with BH-II (Fig. 4), what could have enabled a higher rate of pedogenesis than in BH-II so that the diagnostic horizons could be formed thicker. On the other hand, this difference could also be caused by continuing pedogenesis during the last 3.8 ka in BH-rec: Also the non-humic lower B horizons in transect cores 2–6, not influenced by soil relocation (Fig. 3), are systematically thicker compared with those of buried profiles BH-II and BH-III (the latter profile described in von Suchodoletz et al., 2023). Accordingly, given that the catena includes substrates with different sand contents (see Table S1), the observed systematic differences between the buried and neighboring recent soils in the Bornhöck area should largely be caused by different durations and hence intensities of pedogenesis, i.e. mainly ongoing decalcification in the recent soils. In contrast, given the relic character of Chernozem/Phaeozem formation in Central Germany no systematic increase of the humus-rich upper horizons is visible, and the thickness is typical for regional Chernozems/Phaeozems (Fig. 6). By comparing our values with those from other regional Chernozems/Phaeozems, it appears that decalcification in the Bornhöck area is generally deeper than the regional mean values (Fig. 6). This could be caused by the high sand content in our sandy loess and Saalian moraine compared with Weichselian loess, forming the parent material of the other studied regional Chernozems/Phaeozems (Baumann et al., 1983, Altermann et al., 2005, Dultz and Kühn, 2005, von Suchodoletz et al., 2019). Furthermore, the comparison also reveals that BH-rec, showing the thickest upper humus-rich horizons and the greatest decalcification depth of all recent profiles in the Bornhöck area, seems to form an exception rather than the rule also on the regional scale (Fig. 6).

The current TOC values in both profiles are similar (Fig. 7). However, given that organic matter can be decomposed in well-drained aerobic paleosols (Breuning-Madsen et al., 2009), it is also possible that TOC was originally higher in buried profile BH-II. Accordingly, slightly enhanced Cu contents in the humus-rich upper horizons of BH-II (Fig. 4) may suggest decomposition and mineralisation of organic matter since 3.8 ka, since Cu is a micro-element naturally present in organic matter (Hejcman et al., 2013; Fig. 7).

The contribution of BC to TOC is systematically lower in recent profile BH-rec compared with BH-II, with the lowest values found in the recent Ap horizon (Fig. 7). This effect is also displayed by the significantly lighter colors of the humus-rich upper horizons in BH-rec (Fig. 4). Similarly, lower contributions of BC to TOC in recent compared with buried Neolithic Chernozems/Phaeozems were also formerly observed in Central Germany (von Suchodoletz et al., 2019). In their review of global content and patterns of BC, Reisser et al. (2016) observed a positive correlation between BC and soil pH due to less BC

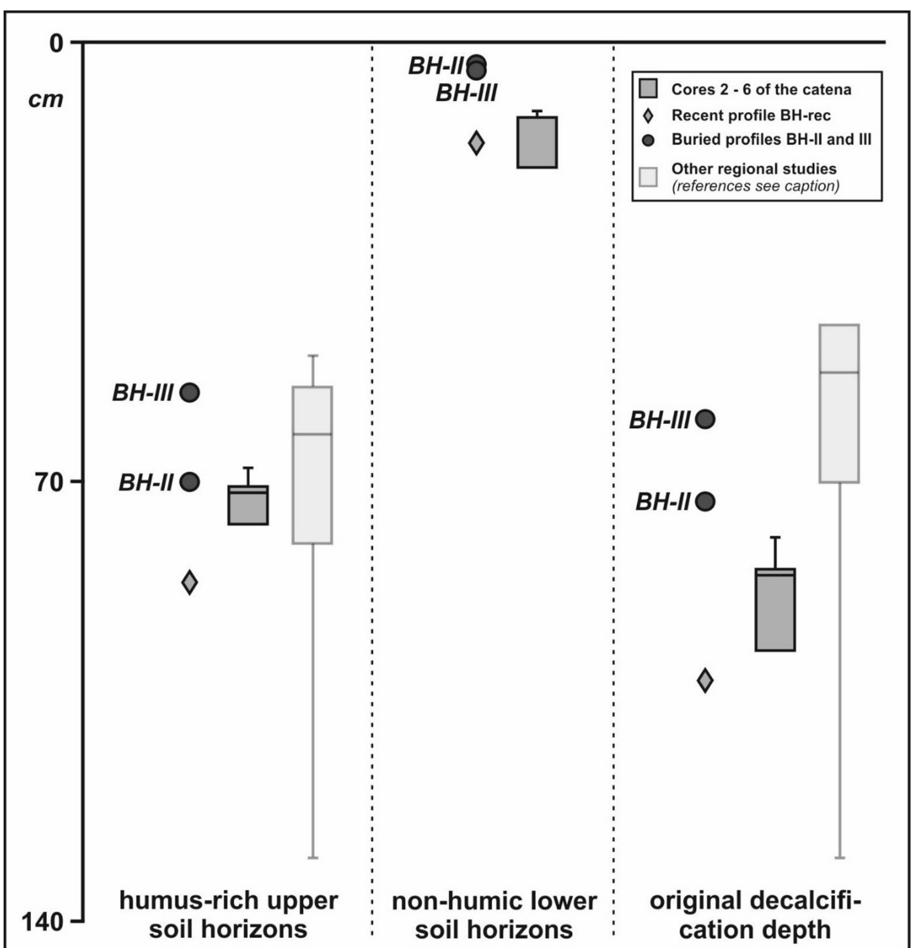

Fig. 6. Thicknesses of the humus-rich upper (A and AB) and non-humic lower (B) soil horizons and original calcification depths (secondary recalcification not taken into account here) of Central German Chernozems/Phaeozems studied in drill cores 2 – 6 of the catena (visibly not influenced by soil erosion or colluviation; Fig. 3), recent profile BH-rec and buried profiles BH-II and BH-III (for the latter see von Suchodoletz et al., 2023), as well as from other regional studies (for those studies no information about non-humic lower soil horizons was available): Altermann et al. (2005: profile Lauchstädt), von Suchodoletz et al. (2019: profiles Neumark-Nord I, Uichteritz I, Zauschwitz), Dultz and Kühn (2005: profile Etzdorf), Baumann et al. (1983: profile Werben).

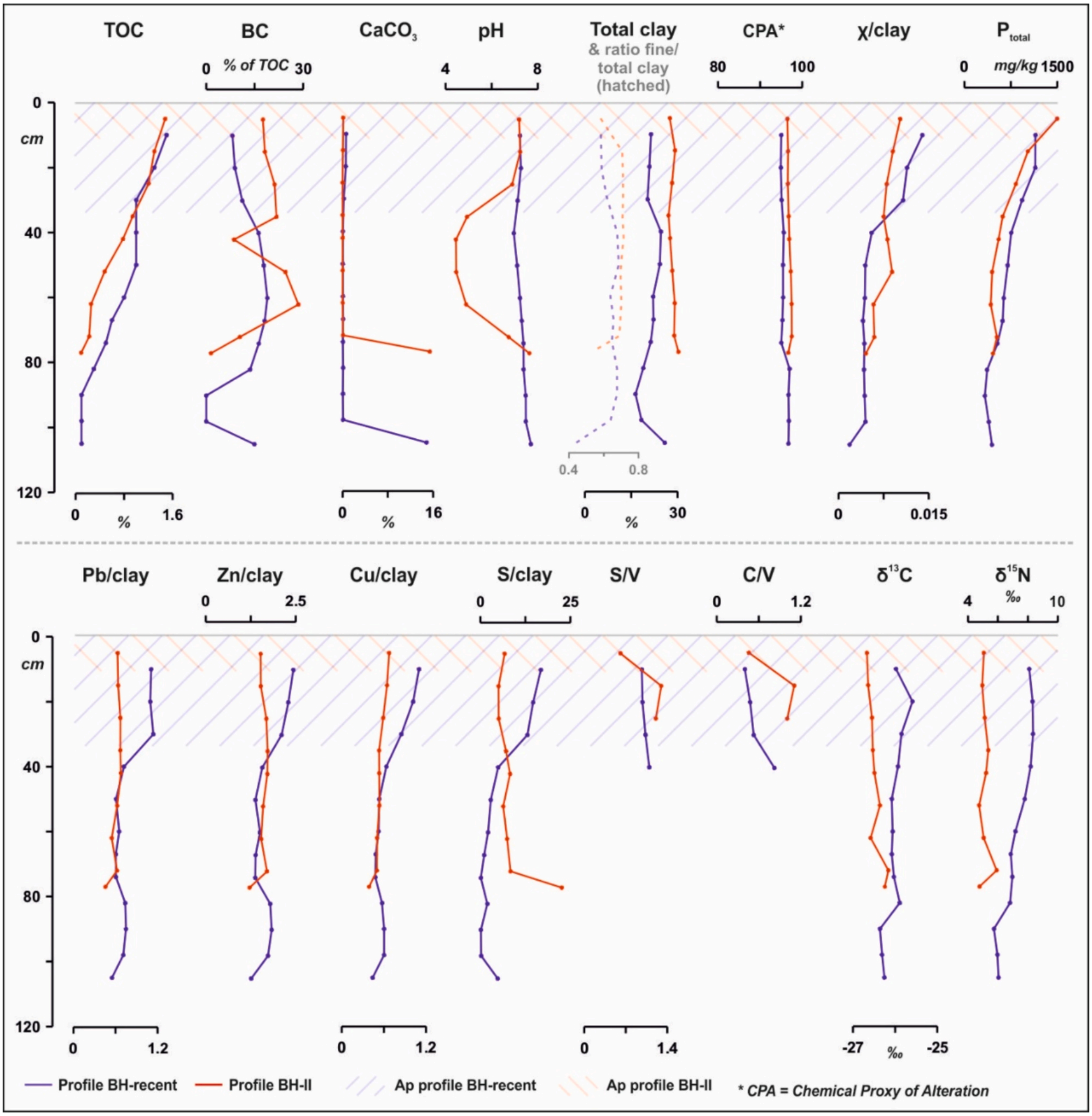

Fig. 7. Comparison of different proxies between recent profile BH-rec and buried profile BH-II. Since the concentration-dependent parameters χ, Pb, Cu, Zn and S show correlations ≥ 0.5 with clay (whereas P_{total} does not), to make both profiles comparable with each other these parameters were related to the clay content.

decomposition at higher soil pH values (i.e. BC metabolization or complete degradation; Gross et al., 2025). Accordingly, we suggest that the higher contributions of BC to TOC in buried Central German Neolithic/Bronze Age Chernozems/Phaeozems should reflect their original BC contents and/or additional BC input due to human fire activities. In contrast, due to ongoing natural decalcification during the last millennia, causing lower pH values and hence increased BC decomposition, systematically lower contributions of BC to TOC are found in recent regional Chernozems/Phaeozems.

Deeper decalcification in BH-rec compared with BH-II (Fig. 6) is displayed by different decalcification depths: The high carbonate content of the parent material (~15 %) is reached in BH-rec at 105 cm, whereas in buried profile BH-II it is already reached at 77 cm. However, small carbonate contents of about 0.5 % are found in upper profile BH-rec (Fig. 7), and calcium carbonate was also detected in the upper parts of all recent cores of the catena (Fig. 3). Together with pH-values ≥ 7 throughout profile BH-rec and in upper profile BH-II, but pH-values down to 4.5 in the central part of BH-II, this indicates regional secondary recalcification that much stronger affected recent profile BH-rec than buried profile BH-II. Secondary recalcification was probably linked with human activity since the industrialization (see Section 5.2). Hence, both profiles should have been largely decalcified and shown acid pH values at latest about 3.8 ka, but decalcification continued only in BH-rec until the start of secondary recalcification during the late 19th century CE (see Section 5.2).

Longer-lasting decalcified conditions in the upper parts of regional soils during the last millennia were also found in other regional Chernozems/Phaeozems (Baumann et al., 1983, von Suchodoletz et al., 2019), and are furthermore indicated by small clay coatings in upper profile BH-rec (sample Rec-MM-I; Fig. 5c). The latter indicate clay translocation that requires pH-values between 4.5 and 6.5 (Quénard et al., 2011). Given that no clay coatings were found by micromorphology in buried profile BH-II and the middle sample of profile BH-rec (Rec-MM-II), clay translocation must have started after burial of profile BH-II about 3.8 ka, and did not have enough time to progress into deeper horizons of profile BH-rec prior to its recalcification. In contrast, small clay coatings in the lowermost sample of BH-rec (Rec-MM-III; Fig. 5f), taken from the Saalian moraine below the stone line (Fig. 4), must originate from a former phase of clay illuviation such as during the Eemian interglacial or the Latest Pleistocene interstadials (Neumeister et al., 1971, Kühn et al., 2006). Accordingly, two small peaks of the ratio fine/total clay at ca. 30–50 cm and 80–90 cm in profile BH-rec encompass the positions of micromorphological samples Rec-MM-I and Rec-MM-III showing small clay coatings, whereas no such peak exists at the position of sample Rec-MM-II without clay coatings (Fig. 7).

The Chemical Proxy of Alteration (CPA) shows similar values between about 95 and 98 throughout both profiles, and slightly higher values in buried profile BH-II compared with the upper part of recent profile BH-rec could reflect slight mineralogical differences between both profiles (Buggle et al., 2011). The high values in both profiles demonstrate (i) no significant regional silicate weathering since about 3.8 ka, and (ii) the composition of the regional soil parent material of already strongly pre-weathered sediments, since unweathered Central German loess shows much lower CPA-values between 84 and 90 (Krauß et al., 2016).

Summing up, the regional Chernozems/Phaeozems were decalcified down to the C horizons about 3.8 ka ago. Since that time decalcification continued, leading to larger thicknesses of the non-humic subsoil horizons. In contrast, the currently observed secondary recalcification of the recent soils was probably caused by human activity during the last decades. Buried and recent soils show similar TOC contents, however, given possible decomposition and mineralization of organic matter in well-drained paleosols (Breuning-Madsen et al., 2009), it cannot be excluded that TOC in the buried soil was higher at 3.8 ka compared with today. Similar with other regional Chernozems/Phaeozems the contribution of BC to TOC became significantly lower since 3.8 ka, possibly also causing the lighter colors of recent soils. BC decomposition must have been caused by acidic conditions during the last millennia (Reisser et al., 2016), leading to a less stable pool of soil organic matter due to a lower proportion of old (historical) BC (Kopecky et al., 2021). Since about 3.8 ka slight clay translocation occurred, proceeding very slowly due to the relatively dry regional climate with mean annual precipitation <600 mm/a (Rogaar et al., 1993). Although the CPA is less sensitive to small-scale differences in weathering intensity at values >85 as found in our study area (Wang et al., 2023), the consistently similar values between both profiles exclude significant silicate mineral weathering during the last millennia. Generally, the high carbonate content of the parent material of about 15 % and the dry regional climate with 550 mm annual precipitation obviously caused only slight soil alteration during the last 3.8 ka. This contrasts with former Chernozems/Phaeozems in other regions of Central Europe that were completely degraded during the last millennia (Kabała et al., 2019, Krupski et al., 2024), such as in parts of southern Poland with higher annual precipitation of about 600–650 mm/a and lower carbonate contents of the regional soil parent material of about 5–6 % (Wiesniewski et al., 2015, 2022, Krawczyk et al., 2017).

5.2. Human overprinting of regional soils

5.2.1. Until and during the Early Bronze Age

The Bornhöck area is located in a region that has agriculturally been used since the Neolithic (Tinapp & Stäuble, 2000). Luminescence dating of buried profile BH-II has revealed a shallow Early Bronze Age Ap horizon, less than 20 cm thick (von Suchodoletz et al., 2023). This depth is typical for Bronze Age plowing, which rarely exceeded 15 cm depth (Pavelka et al., 2017, Scherer et al., 2021). S/V-ratios around 1.2 and C/V-ratios around 1.0 indicate that grass-dominated vegetation existed at site BH-II before it was buried during the Early Bronze Age (Thevenot et al., 2010). Previous research suggested that the regional natural pre-Neolithic Holocene vegetation consisted of pine forests interspersed with non-forested habitats (Litt, 1992, von Suchodoletz et al., 2024, Tinapp et al., 2025). Hence, the applied vegetation proxy may reflect either a local pre-Neolithic non-forested habitat, and/or a subsequent cereal-related signal associated with farming activities prior to the construction of the burial mound. These crops were likely dominated by barley, emmer and spelt as found at other western-central European sites for that time (Stika & Heiss, 2014). Furthermore, the high P_{total} content in the Early Bronze Age Ap horizon (Figs. 4 and 7) may have been caused by fertilization, cattle breeding or local waste disposal during that time (Holliday & Gartner, 2007). The $\delta^{13}C$ values (−26.2 ‰ to −26.7 ‰) fall within the typical range for C3 plants (−29 ‰ and −25 ‰, O'Leary 1988, O'Leary et al., 1992), reflecting both the natural pre-Neolithic vegetation and the subsequently cultivated crops. Notably, millet, a first C4 crop in this area, only arrived later in the Bronze Age (Filipovic et al., 2020), i.e. after the burial mound was constructed. The $\delta^{15}N$ values of 4.8 ‰ to 5.9 ‰ most probably reflect the natural $\delta^{15}N$ level of the Chernozem, and do not necessarily indicate human dung management (Schlütz et al., 2023).

Beyond these observations, no further human influence was detected in the buried Chernozem. This aligns with broader patterns, as human impact on Central European landscapes during the Early Bronze Age was rather limited (Zapolska et al., 2023).

5.2.2. Since the Early Bronze Age

With a thickness of 34 cm the Ap horizon of profile BH-rec is much deeper than that of profile BH-II, corresponding with typical depths observed in present-day Ap horizons in Central Europe (Schatz, 2023). Additionally, features of soil erosion and colluviation processes are documented in the catena (Fig. 3). Although our study did not resolve their exact chronology, it is most likely that these processes occurred primarily since the Early Bronze Age (Dotterweich, 2008, Dreibrodt et al., 2013).

Furthermore, aside from a possible slight increase in P_{total}, the recent Ap horizon shows enrichments of the elements Pb, Zn, Cu and S as well as higher magnetic susceptibility χ (Figs. 4). Yet, the absolute values of these elements, which show a significant correlation with clay content (see Fig. S-1), remain within the range of the geological background of the more clay-rich profile BH-II. When normalized to clay content their relative enrichment in the recent Ap becomes much more apparent (Fig. 7). Unlike phosphorous, these enrichments cannot be attributed to agricultural activities. The region has been strongly industrialized since the end of the 19th century CE, with lignite burning serving as the major energy source until the early 1990s (Neumeister et al., 1991). While smaller sources existed especially in larger settlements due to industrial and domestic heating, the major contributors were lignite power plants, which emitted large amounts of lignite ash (Fig. 8). In 1989 alone, approximately 4.9 Mio. t of lignite ash were released (Zikeli et al., 2002). Wind carried this fly ash over a large area, depositing variable amounts of elements such as Mn, Cr, Zn, Cu, Pb, V and Ni (Neumeister et al., 1991; Fig. 8). This likely explains the enrichment of the heavy metals, particularly Pb, Zn and Cu, in the recent Ap horizon. Ferrimagnetic magnetite particles, produced during burning of pyrite-rich lignite, are responsible for increased values of magnetic susceptibility (Rumpel et al., 1998). Hence, this could account for the relative increase of χ in the recent Ap horizon. The relatively low human enrichment of heavy metals and magnetic particles in the recent soils of the Bornhöck area, despite their location within the Central German industrial region, can likely be attributed to their distance from lignite power plants and large settlements which were the primary sources of fly ash emissions (Fig. 8).

Lignite ash is also enriched in sulphur and calcium (Fig. 8), with the

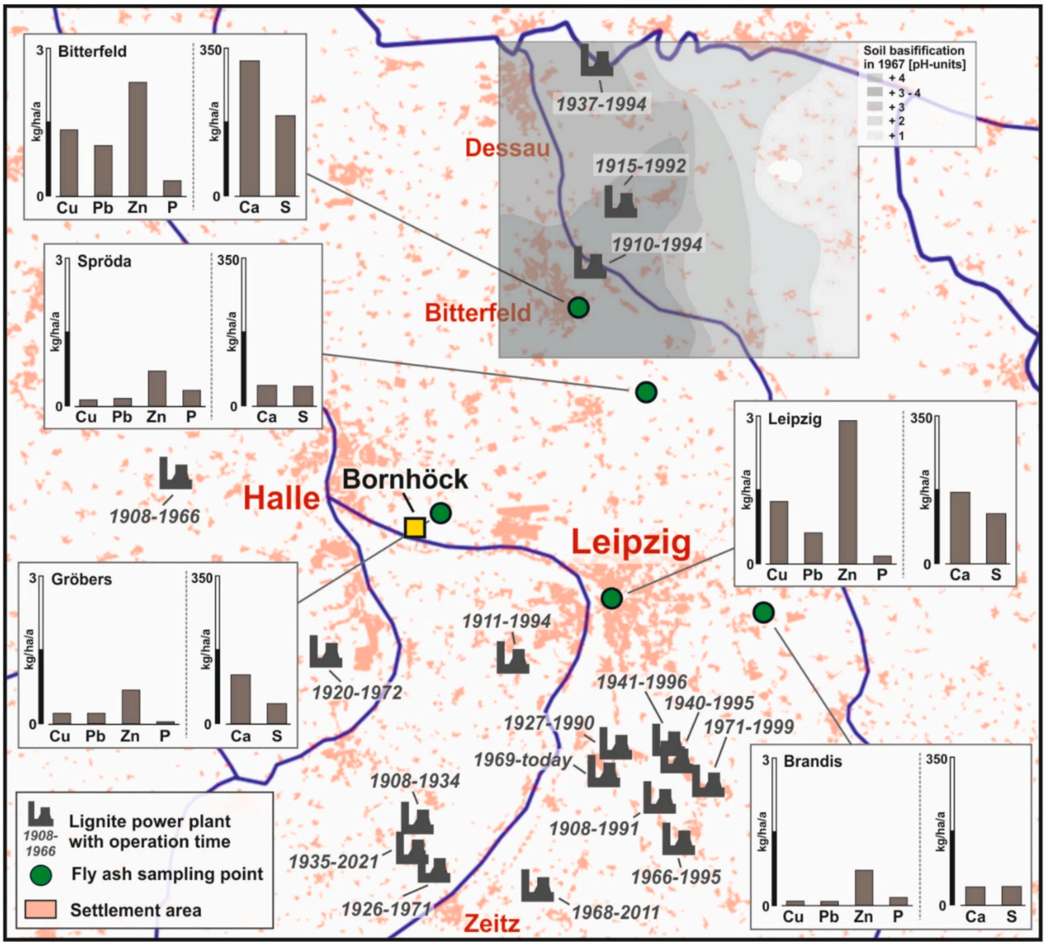

Fig. 8. Lignite power plants that were active prior to 1990 with operation times (LMBV, 2011, 2019), settlements and fly ash sampling points with elemental analyses (Neumeister et al., 1991) in the Central German industrial region, and location of the Bornhöck. (Settlements: ©GeoBasis-DE/BKG 2022, Rivers: @Naturalearthdata). Furthermore, for the northeastern part (Düben Heath) soil basification in 1967 due to fly ash input compared with natural values is shown (Konopatzky et al., 1995).

latter contributing to pH-values > 7 in fly ash and promoting secondary carbonate precipitation in regional soils formed on fly ash deposits (Zikeli et al., 2002). This likely explains the observed S-enrichment in the recent Ap horizon, the alkaline pH-values throughout profile BH-rec and in upper part of profile BH-II, as well as the secondary carbonate precipitation in upper part of profile BH-rec, the catena (Fig. 3) and, to a much lower extent, in uppermost profile BH-II. As discussed by Körschens et al. (2005), fly ash deposition appears to have led to the recalcification of some regional soils, transforming previously decalcified soils with minor features of clay illuviation into calcic Chernozems/Phaeozems while still preserving their luvic properties. Likewise, in 1967 strong basification of regional soils due to fly ash input was systematically documented for the Düben Heath located northeast of the Bornhöck area (Konopatzky et al., 1995; Fig. 8).

These altered chemical properties inhibit transformation processes such as clay relocation and BC-decomposition (Fischer-Zujkov, 1999, Semmel, 1995, Reisser et al., 2016), and impact soil biota (Aciego Pietri & Brookes, 2008, Thies & Grossmann, 2023). The intensive alkalinization and secondary calcification of soils nearby former lignite power plants – caused by fly ash deposition – strongly contrasts to the more widespread effects of industrial lignite burning, where atmospheric SO_2 input led to soil acidification and contributed to large-scale forest dieback in the second half of the 20th century CE (Wetstone & Foster, 1983, Šramek et al., 2008).

Under Holocene climate conditions, the anthropogenically recalcified Central German Chernozems/Phaeozems would typically undergo decalcification processes again in the mid-term future. However, given the current climate change with rising regional temperature (Kaspar et al., 2023) and an increasing regional annual water deficit in the already currently dry region (Zink et al., 2017), decalcification should strongly decelerate or even stop.

Unlike profile BH-II, which showed a dominance of grass vegetation before burial, S/V-values around 1.0 and C/V-values between 0.4 and 0.8 in recent profile BH-rec suggest a mix of grasses and deciduous trees (Thevenot et al., 2010). This indicates that, despite intensive agricultural use since the Neolithic, deciduous trees possibly related to the current potential natural vegetation of *Quercus-Carpinus* forests with minor *Fagus* proportions (Bohn & Weiß 2003) must have grown at this site at some point over the past 3.8 ka. Although within the range of C3 plants, the $\delta^{13}C$ values in upper profile BH-rec reach up to −25.6 ‰, i.e. about 1 ‰ higher than those in buried profile BH-II (Fig. 7). This difference may result from the recent cultivation of the C4 crop maize, which has been part of the crop rotation for at least 30 years (local farmer, oral communications). Elevated $\delta^{15}N$ values of >8 ‰ in upper profile BH-rec could be caused by current manuring practices using organic remains from a biogas plant. Similar to animal dung, microbial activity in biogas plants encompasses release of ^{14}N enriched volatile gases, raising the $\delta^{15}N$ of the remaining decomposed organic matter (Fry, 2008, Bell et al., 2016, Pedersen and Hafner, 2023). This increase in $\delta^{15}N$ appears to extend down to about 80 cm, i.e. the lower boundary of the black-colored soil horizons (Fig. 4).

In summary, the recent regional Chernozems/Phaeozems are much stronger influenced by human activity compared to the buried Bronze Age soil. Key anthropogenic impacts include: (i) Industrialization-era fly ash deposition, which led to increased magnetic susceptibility, heavy metal and sulfur enrichment, and secondary recalcification. (ii) Modern agricultural activity, which altered the isotopic signature of soil organic matter. Our study highlights the value of directly comparing neighboring recent soils and buried paleosols, allowing the clear identification of recent and sub-recent human impact not biased by largely different sedimentological, pedological and geochemical backgrounds (Reimann & Garrett, 2005, Pampura et al., 2019). This is particularly relevant for detecting smaller-scale human effects such as moderate enrichment of heavy metals and higher values of magnetic susceptibility in recent soils, which could otherwise be overlooked. Interestingly, the approximately 70–80 cm of archaeosediments that remained over profile BH-II after mound destruction during the second half of the 19th century CE appear to have largely protected the paleosol from younger soil forming processes. Furthermore, despite intensive agricultural use, the recent soils still contain a potential Late Holocene vegetation signal, highlighting their valuable potential as geoarchives even in intensively farmed landscapes.

6. Conclusion

By comparing a buried Chernozem beneath a Late Bronze burial mound with a neighboring similar surface soil, we systematically studied natural Chernozem/Phaeozem alterations and human overprinting in the Central German industrial region over the past 3.8 ka. While similar comparisons have been conducted in regions such as East-Central and Eastern Europe or Denmark, they have been largely overlooked in this area. Unlike in more humid regions with less calcareous soil parent material where former Chernozems/Phaeozems have been completely transformed to Luvisols during the last millennia, our findings indicate a slow transformation of regional Chernozems/Phaeozems since approximately 3.8 ka. This is likely due to the dry regional climate and the high carbonate contents of the soil parent material. This transformation manifests primarily as ongoing decalcification, BC decomposition and weak clay illuviation processes.

Consistent with previous studies from Central Europe, human influence on the soils was minor before and during the Early Bronze Age, limited mainly to <20 cm thick local plough horizons and some P enrichment possibly due to agricultural activity or local waste disposal. In contrast, human impact has increased since the late 19th century CE. This is evident in the enrichment of magnetic susceptibility, heavy metals and sulfur likely due to fly ash input from lignite power plants, as well as in shifts in the isotopic signature of soil organic matter caused by modern agriculture. However, given the study site's remote location from major fly ash sources, these enrichments remain moderate and might have been overlooked without a systematic comparison between buried and recent soils.

However, the strongest human impact on regional soils was their secondary recalcification by fly ash input, which has led to alkaline pH values in previously decalcified soils. This process halted the natural transformation from Chernozems/Phaeozems to Luvisols, and changed the conditions for soil biota. Generally, in the context of ongoing climate change with increasing regional temperatures decalcification should strongly decelerate or even stop, what should also influence long-term future soil formation processes and ecosystem dynamics.

CRediT authorship contribution statement

Hans von Suchodoletz: Writing – review & editing, Writing – original draft, Validation, Formal analysis, Data curation, Conceptualization. **Birgit Schneider:** Writing – review & editing, Writing – original draft, Validation, Methodology, Investigation, Formal analysis, Data curation. **Anna Skokan:** Writing – review & editing, Writing – original draft, Investigation, Formal analysis, Data curation. **Teresa Nitz:** Writing – review & editing, Writing – original draft, Investigation, Formal analysis, Data curation. **Bruno Glaser:** Writing – review & editing, Writing – original draft, Validation, Methodology, Investigation, Formal analysis, Data curation. **Steven Polivka:** Writing – review & editing, Writing – original draft, Investigation, Conceptualization. **Katja Wiedner:** Writing – review & editing, Writing – original draft, Investigation, Formal analysis, Data curation, Conceptualization. **Frank Schlütz:** Writing – review & editing, Writing – original draft, Validation, Methodology, Investigation, Formal analysis, Data curation. **Torsten Schunke:** Writing – review & editing, Writing – original draft, Validation, Resources. **Peter Kühn:** Writing – review & editing, Writing – original draft, Validation, Methodology, Investigation, Formal analysis, Data curation.

Declaration of competing interest

The authors declare the following financial interests/personal relationships which may be considered as potential competing interests: Frank Schluetz reports financial support was provided by German Research Foundation. If there are other authors, they declare that they have no known competing financial interests or personal relationships that could have appeared to influence the work reported in this paper.

Acknowledgements

We thank the Gut Rohlmann & Gröbers GbR for allowing uncomplicated access to their agricultural fields and giving information about their agricultural practices, as well as Katja Pöhlmann (Leipzig) and Heike Maennicke (Halle) for their help during laboratory analysis. The isotope analyses were funded by the Deutsche Forschungsgemeinschaft (DFG) under Germany's Excellence Strategy – EXC 2150 – 390870439.

Appendix A. Supplementary data

Supplementary data to this article can be found online at https://doi.org/10.1016/j.catena.2025.109270.

Data availability

Analytical data of a buried and a recent surficial Chernozem in the Bornhöck area in Central Germany (Original data) (PANGAEA)

References

Aciego Pietri, J.P., Brookes, P.C., 2008. Relationships between soil pH and microbial properties in a UK arable soil. Soil Biol. Biochem. 40, 1856–1861. https://doi.org/10.1016/j.soilbio.2008.03.020.

Acksel, A., Kappenberg, A., Kühn, P., Leinweber, P., 2017. Human activity formed deep, dark topsoils around the Baltic Sea. Geoderma Reg. 10, 93–101. https://doi.org/10.1016/j.geodrs.2017.05.005.

Adhikari, K., Hartemink, A.E., 2016. Linking soils to ecosystem services—A global review. Geoderma 262, 101–111. https://doi.org/10.1016/j.geoderma.2015.08.009.

Alexandrovskiy, A.L., Sedov, S., Shishkov, V.A., 2014. The development of deep soil processes in ancient kurgans of the North Caucasus. Catena 112, 65–71. https://doi.org/10.1016/j.catena.2013.03.014.

Altermann, M., Rinklebe, J., Merbach, I., Körschens, M., Langer, U., Hoffmann, B., 2005. Chernozem - soil of the year 2005. J. Plant Nutr. Soil Sci. 168, 725–740. https://doi.org/10.1002/jpln.200521814.

Amelung, W., Martius, C., Bandeira, A.G., Garcia, M.V.B., Zech, W., 2002. Lignin characteristics and density fractions of termite nests in an amazonian rain forest—Indicators of termite feeding guilds? Soil Biol. Biochem. 34, 367–372. https://doi.org/10.1016/S0038-0717(01)00192-4.

Barczi, A., Nagy, V., 2016. Kurgans: markers of the holocene climatic change(s). Analecta 10, 47–52. https://doi.org/10.14232/analecta.2016.1.47-52.

Baumann, W., Fritzsche, C., Coblenz, W., Fiedler, H.J., Brückner, H.-P., 1983. Stratigraphische Befunde zur Schnurkeramik in einem Grabhügel bei Werben, Kr. Leipzig. Ausgrabungen und Funde 28, 1–10.

Bell, M.W., Tang, Y.S., Dragosits, U., Flechard, C.R., Ward, P., Braban, C.F., 2016. Ammonia emissions from an anaerobic digestion plant estimated using atmospheric

measurements and dispersion modelling. Waste Manag. 56, 113–124. https://doi.org/10.1016/j.wasman.2016.06.002.
Bohn, U., Welß, W., 2003. Die potenzielle natürliche Vegetation. In: Nationalatlas Bundesrepublik Deutschland, Natur und Umwelt II: Klima, Pflanzen- Und Tierwelt, vol. 3. Leibniz Institut für Länderkunde, Leipzig, pp. 84–87.
Breuning-Madsen, H., Elberling, B., Balstroem, T., Holst, M., Freudenberg, M., 2009. A comparison of soil organic carbon stock in ancient and modern land use systems in Denmark. Eur. J. Soil Sci. 60, 55–63. https://doi.org/10.1111/j.1365-2389.2008.01089.x.
Brigand, R., Weller, O., 2013. Neolithic and chalcolithic settlement patterns in Central Moldavia (Romania). Doc. Praehist. 40, 195–207. https://doi.org/10.4312/dp.40.15.
Brodowski, S., Rodionov, A., Haumaier, L., Glaser, B., Amelung, W., 2005. Revised black carbon assessment using benzene polycarboxylic acids. Org. Geochem. 36, 1299–1310. https://doi.org/10.1016/j.orggeochem.2005.03.011.
Bruckmeier, K., Grund, H., 1994. Perspectives for environmentally sound agriculture in East Germany. In: Symes, D., Jansen, A.J. (Eds.), Agricultural Restructuring and Rural Change in Europe. Wageningen University Press, Wageningen, pp. 180–194.
Buggle, B., Glaser, B., Hambach, U., Gerasimenko, N., Marković, S., 2011. An evaluation of geochemical weathering indices in loess-paleosol studies. Quat. Int. 240, 12–21. https://doi.org/10.1016/j.quaint.2010.07.019.
Chesworth, W. (Ed.), 2016. Encyclopedia of Soil Science. Springer. Dordrecht, Berlin, Heidelberg, New York.
Dotterweich, M., 2008. The history of soil erosion and fluvial deposits in small catchments of central Europe: Deciphering the long-term interaction between humans and the environment — a review. Geomorphology 101, 192–208. https://doi.org/10.1016/j.geomorph.2008.05.023.
Dreibrodt, S., Jarecki, H., Lubos, C., Khamnueva, S.V., Klamm, M., Bork, H.-R., 2013. Holocene soil formation and soil erosion at a slope beneath the Neolithic earthwork Salzmünde (Saxony-Anhalt, Germany). Catena 107, 1–14. https://doi.org/10.1016/j.catena.2013.03.002.
Dreibrodt, S., Hofmann, R., dal Corso, M., Bork, H.-R., Duttmann, R., Martini, S., Saggau, P., Schwark, L., Shatilo, L., Videiko, M., Nadeau, M.-J., Grootes, P.M., Kirleis, W., Müller, J., 2022. Earthworms, Darwin and prehistoric agriculture - Chernozem genesis reconsidered. Geoderma 409, 115607. https://doi.org/10.1016/j.geoderma.2021.115607.
Dreibrodt, S., Langan, C.C.M., Fuchs, M., Bork, H.-R., 2023. Anthropogenic impact on erosion, pedogenesis and fluvial processes in the central European landscapes of the eastern Harz mountains forelands (Germany). Quat. Sci. Rev. 303, 107980. https://doi.org/10.1016/j.quascirev.2023.107980.
Dror, I., Yaron, B., Berkowitz, B., 2022. The human impact on all soil-forming factors during the Anthropocene. ACS Environ. Au 2, 11–19. https://doi.org/10.1021/acsenvironau.1c00010.
Dultz, P., Kühn, P., 2005. Occurrence, formation, and micromorphology of gypsum in soils from the Central-German Chernozem region. Geoderma 129, 230–250. https://doi.org/10.1016/j.geoderma.2005.01.022.
Eckmeier, E., Gerlach, R., Gehrt, E., Schmidt, M.W.I., 2007. Pedogenesis of Chernozems in Central Europe - a review. Geoderma 139, 288–299. https://doi.org/10.1016/j.geoderma.2007.01.009.
Eissmann, L., 2002. Quaternary geology of eastern Germany (Saxony, Saxon-Anhalt, South Brandenburg, Thüringia), type area of the Elsterian and Saalian stages in Europe. Quat. Sci. Rev. 21, 1275–1346. https://doi.org/10.1016/S0277-3791(01)00075-0.
Filipović, D., Meadows, J., Dal Corso, M., Kirleis, W., Alsleben, A., Akeret, Ö., Bittmann, F., Bosi, G., Ciută, B., Dreslerová, D., Effenberger, H., Gyulai, F., Heiss, A. G., Hellmund, M., Jahns, S., Jakobitsch, T., Kapcia, M., Klooß, S., Kohler-Schneider, M., Kroll, H., Makarowicz, P., Marinova, E., Märkle, T., Medović, A., Mercuri, A.M., Mueller-Bieniek, A., Nisbet, R., Pashkevych, G., Perego, R., Pokorný, P., Pospieszny, Ł., Przybyła, M., Reed, K., Rennwanz, J., Stika, H.-P., Stobbe, A., Tolar, T., Wasylikowa, K., Wiethold, J., Zerl, T., 2020. New AMS ^{14}C dates track the arrival and spread of broomcorn millet cultivation and agricultural change in prehistoric Europe. Sci. Rep. 10, 13698. https://doi.org/10.1038/s41598-020-70495-z.
Fischer-Zujkov, U., 1999. Schwarzerdeähnliche Böden des Jungmoränengebietes. ZALF-Bericht 37, 26–56.
Fry, B., 2008. Stable isotope ecology, first ed. Springer, New York.
Gerlach, R., Fischer, P., Eckmeier, E., Hilgers, A., 2012. Buried dark soil horizons and archaeological features in the Neolithic settlement region of the lower Rhine area, NW Germany: Formation, geochemistry and chronostratigraphy. Quat. Int. 265, 191–204. https://doi.org/10.1016/j.quaint.2011.10.007.
Glaser, B., Haumaier, L., Guggenberger, G., Zech, W., 1998. Black carbon in soils: the use of benzenecarboxylic acids as specific markers. Org. Geochem. 29, 811–819. https://doi.org/10.1016/S0146-6380(98)00194-6.
Goñi, M.A., Hedges, J.I., 1992. Lignin dimers: Structures, distribution, and potential geochemical applications. Geochim. Cosmochim. Acta 56, 4025–4043. https://doi.org/10.1016/0016-7037(92)90014-A.
Gross, A., Solic, M., Glaser, B., Bromm, T., Maletic, S., 2025. Relevance of biochar metabolization - evidence from a long-term biochar field experiment. Front. Sustain. Food Syst. 9. https://doi.org/10.3389/fsufs.2025.1578363.
Hedges, J.I., Ertel, J.R., 1982. Characterization of lignin by gas capillary chromatography of cupric oxide oxidation products. Anal. Chem. 54, 174–178. https://doi.org/10.1021/ac00239a007.
Hejcman, M., Součková, K., Krištuf, P., Peška, J., 2013. What questions can be answered by chemical analysis of recent and paleosols from the Bell Beaker barrow (2500–2200 BC), Central Moravia, Czech Republic? Quat. Int. 316, 179–189. https://doi.org/10.1016/j.quaint.2013.06.014.
Henkner, J., Ahlrichs, J., Fischer, E., Fuchs, M., Knopf, T., Rösch, M., Scholten, T., Kühn, P., 2018. Land use dynamics derived from colluvial deposits and bogs in the Black Forest, Germany. J. Plant Nutr. Soil Sci. 181, 240–260. https://doi.org/10.1002/jpln.201700249.
Hildebrandt-Radke, I., Makarowicz, P., Matviishyna, Z., Parkhomenko, A., Lysenko, S.D., Kochkin, I.T., 2019. Late Neolithic and Middle Bronze Age barrows in Bukivna, Western Ukraine as a source to understand soil evolution and its environmental significance. J. Archaeol. Sci. Rep. 27, 101972. https://doi.org/10.1016/j.jasrep.2019.101972.
Holliday, V.T., Gartner, W.G., 2007. Methods of soil P analysis in archaeology. J. Archaeol. Sci. 34, 301–333. https://doi.org/10.1016/j.jas.2006.05.004.
IUSS Working Group WRB, 2022. World Reference Base for Soil Resources. International Soil Classification System for Naming Soils and Creating Legends for Soil Maps, 4th edition. International Union of Soil Sciences (IUSS), Vienna, Austria.
Jenny, H., 1994. Factors of soil formation. Dover Publications, New York.
Kabała, C., Przybył, A., Krupski, M., Łabaz, B., Waroszewski, J., 2019. Origin, age and transformation of Chernozems in northern Central Europe - New data from Neolithic earthen barrows in SW Poland. Catena 180, 83–102. https://doi.org/10.1016/j.catena.2019.04.014.
Kasielke, T., Poch, R.M., Wiedner, K., 2019. Chernozem relics in the Hellweg Loess Belt (Westphalia, NW Germany) - Natural or man-made? Quat. Int. 502B, 296–308. https://doi.org/10.1016/j.quaint.2018.09.015.
Kaspar, F., Friedrich, K., Imbery, F., 2023. Observed temperature trends in Germany: current status and communication tools. Meteorol. Z. 32, 279–291. https://doi.org/10.1127/metz/2023/1150.
Keesstra, S.D., Bouma, J., Wallinga, J., Tittonell, P., Smith, P., Cerdà, A., Montanarella, L., Quinton, J.N., Pachepsky, Y., van der Putten, W.H., Bardgett, R.D., Moolenaar, S., Mol, G., Jansen, B., Fresco, L.O., 2016. The significance of soils and soil science towards realization of the United Nations sustainable development goals. Soil 2, 111–128. https://doi.org/10.5194/soil-2-111-2016.
Khokhlova, O.S., Khokhlov, A., Oleynik, S.A., Gabuev, T.A., Malashev, V.Y., 2007. Paleosols from the groups of burial mounds provide paleoclimatic records of centennial to intercentennial time scale: a case study from the Early Alan cemeteries in the Northern Caucasus (Russia). Catena 71, 477–486. https://doi.org/10.1016/j.catena.2007.03.013.
Koch, J., Klose, S., Makeschin, F., 2002. Stratigraphic and spatial differentiation of chemical properties in long-term fly ash influenced forest soils in the Dübener Heide region, NE Germany. Forstl. Cent.bl. 121, 157–170. https://doi.org/10.1046/j.1439-0337.2002.02027.x.
Konopatzky, A., Kopp, D., Heymann, G., Köhler, S., Kümmel, G., Freyer, C., 1995. Bodenzustandswandel forstlich genutzter Standorte des Immissionsgebietes Dübener Heide und seine Erfassung über die forstliche Standortskartierung. Mitt. Dtsch. Bodenkdl. Ges. 77, 95–124.
Kopecký, M., Kolař, L., Váchalova, R., Konvalina, P., Batt, J., Mráz, P., Menšik, L., Nghia Hoang, T., Dumbrovský, M., 2021. Black carbon and its effect on carbon sequestration in soil. Agronomy 11, 2261. https://doi.org/10.3390/agronomy11112261.
Körschens, M., Altermann, M., Merbach, I., Rinklebe, J., 2005. Böden als unsere Lebensgrundlage – Schwarzerde ist der Boden des Jahres 2005. https://boden-des-jahres.de/wp-content/uploads/2014/09/2005_Festvortrag.pdf (accessed 20 October 2024).
Kottek, M., Grieser, J., Beck, C., Rudolf, B., Rubel, F., 2006. World map of the Köppen-Geiger climate classification updated. Meteorol. Z. 15, 259–263. https://doi.org/10.1127/0941-2948/2006/0130.
Krauß, L., Zens, J., Zeeden, C., Schulte, P., Eckmeier, E., Lehmkuhl, F., 2016. A multi-proxy analysis of two loess-paleosol sequences in the northern Harz foreland, Germany. Palaeogeogr. Palaeoclimatol. Palaeoecol. 46, 401–417. https://doi.org/10.1016/j.palaeo.2016.09.001.
Krawczyk, M., Ryzner, K., Skurzynski, J., Jary, Z., 2017. Lithological indicators of loess sedimentation of SW Poland. Contemp. Trends Geosci. 6, 94–111. https://doi.org/10.1515/ctg-2017-0008.
Krupski, M., Kabała, C., Mackiewicz, M., Sady-Bugajska, A., Tietz, B., Dudek, M., 2024. Investigating soils of barrows in the Rozumice Forest (SW Poland) - Dynamics of soil and landscape evolution in a central European loess plateau. J. Archaeol. Sci. Rep. 58, 104722. https://doi.org/10.1016/j.jasrep.2024.104722.
Kühn, P., Billwitz, K., Bauriegel, A., Kühn, D., Eckelmann, W., 2006. Distribution and genesis of Fahlerden (Albeluvisols) in Germany. J. Plant Nutr. Soil Sci. 169, 420–433. https://doi.org/10.1002/jpln.200521963.
Kühn, P., Lehndorff, E., Fuchs, M., 2017. Lateglacial to Holocene pedogenesis and formation of colluvial deposits in a loess landscape of Central Europe (Wetterau, Germany). Catena 154, 118–135. https://doi.org/10.1016/j.catena.2017.02.015.
Lehmkuhl, F., Nett, J.J., Pötter, S., Schulte, P., Sprafke, T., Jary, Z., Antoine, P., Wacha, L., Wolf, D., Zerboni, A., Hošek, J., Marković, S.B., Obreht, I., Sümegi, P., Veres, D., Zeeden, C., Boemke, B., Schaubert, V., Viehweger, J., Hambach, U., 2021. Loess landscapes of Europe – Mapping, geomorphology, and zonal differentiation. Earth Sci. Rev. 215, 103496. https://doi.org/10.1016/j.earscirev.2020.103496.
Leopold, M., Hürkamp, K., Völkel, J., Schmotz, K., 2011. Black soils, sediments and brown calcic luvisols: a pedological description of a newly discovered Neolithic ring ditch system at Stephansposching, Eastern Bavaria. Germany. Quat. Int. 243, 293–304. https://doi.org/10.1016/j.quaint.2010.11.021.
LGBSA, 1995. Übersicht der Böden von Sachsen-Anhalt 1: 400.000. Landesamt für Geologie und Bergwesen Sachsen-Anhalt, Halle/Saale.
Liedtke, H., Marschner, B., 2003. Bodengüte der landwirtschaftlichen Nutzflächen. In: Nationalatlas Deutschland, Volume 2: Relief, Boden. Wasser. Leibniz Institut für Länderkunde, Leipzig, pp. 104–105.

Lisetskii, F.N., Goleusov, P.V., Chepelev, O.A., 2013. The development of chernozems on the Dniester-Prut interfluve in the Holocene. Eurasian Soil Sci. 46, 491–504. https://doi.org/10.1134/S1064229313050086.

Litt, T., 1992. Fresh investigations into the natural and anthropogenically influenced vegetation of the earlier Holocene in the Elbe-Saale Region, Central Germany. Veg. Hist. Archaeobot. 1, 69–74. https://doi.org/10.1007/BF00206086.

Liu, X., Burras, C.L., Kravchenko, Y.S., Duran, A., Huffman, T., Morras, H., Studdert, G., Zhang, X., Cruse, R.M., Yuan, X., 2012. Overview of mollisols in the world: distribution, land use and management. Can. J. Soil Sci. 92, 383–402. https://doi.org/10.4141/cjss2010-05.

LMBV, 2011. Braunkohlenveredlung in Mitteldeutschland. Teil II (Süd). Mitteldeutsches Braunkohlenrevier, Wandel und Perspektiven 11. Senftenberg.

LMBV, 2019. Braunkohlenveredlung in Mitteldeutschland. Teil I (Nord). Mitteldeutsches Braunkohlenrevier, Wandel und Perspektiven 10. Senftenberg.

Lorz, C., Saile, T., 2011. Anthropogenic pedogenesis of chernozems in Germany?—A critical review. Quat. Int. 243, 273–279. https://doi.org/10.1016/j.quaint.2010.11.022.

Manz, M., Wenzel, K.-D., Dietze, U., Schüürmann, G., 2001. Persistent organic pollutants in agricultural soils of central Germany. Sci. Total Environ. 277, 187–198. https://doi.org/10.1016/S0048-9697(00)00877-9.

Meller, H., Schunke, T., 2016. Die Wiederentdeckung des Bornhöck - Ein neuer frühbronzezeitlicher Fürstengrabhügel bei Raßnitz, Saalekreis. Erster Vorbericht. In: Meller, H., Risch, R., Jung, R. (Eds.), Rich and Poor—Competing for Resources in Prehistoric Societies. Tagungen des Landesmuseums für Vorgeschichte Halle 14, Halle, pp. 227–265.

Meharg, A.A., Meharg, C., 2021. The pedosphere as a sink, source, and record of anthropogenic and natural arsenic atmospheric deposition. Environ. Sci. Technol. 55, 7757–7769. https://doi.org/10.1021/acs.est.1c00460.

Möller, A., Kaiser, K., Zech, W., 2002. Lignin, carbohydrate, and amino sugar distribution and transformation in the tropical highland soils of northern Thailand under cabbage cultivation, pinus reforestation, secondary forest, and primary forest. Soil Res. 40, 977–998. https://doi.org/10.1071/SR01030.

Neumeister, H., 1971. Jungpleistozäne Decksedimente und Bodenentwicklung in der Umgebung von Leipzig. Zpravy Geografickeho Ustavu CSAV 23–72.

Neumeister, H., Franke, C., Nagel, C., Peklo, G., Zierath, R., Peklo, P., 1991. Immissionsbedingte Stoffeinträge aus der Luft als geomorphologischer Faktor. Geoökodynamik 12, 1–40.

O'Leary, M.H., 1988. Carbon isotopes in photosynthesis: Fractionation techniques may reveal new aspects of carbon dynamics in plants. Bioscience 38, 328–336. https://doi.org/10.2307/1310735.

O'Leary, M.H., Madhavan, S., Paneth, P., 1992. Physical and chemical basis of carbon isotope fractionation in plants. Plant Cell Environ. 15, 1099–1104. https://doi.org/10.1111/j.1365-3040.1992.tb01660.x.

Pampura, T., Meili, M., Holm, K., Candaudap, F., Probst, A., 2019. Buried paleosols as reference objects for assessing the current level of soil pollution with lead in the lower Volga Steppes. Agric. Chem./Agrokhimiya 52, 34–49. https://doi.org/10.1134/S1064229319010113.

Pavelka, J., Smetanova, A., Rejman, J., Kovacik, P., 2017. An interdisciplinary tillage erosion experiment: establishing a new field in grasslands with reconstructed ard plough of the Bronze Age–Iron Age. Cuad. Investig: Geogr. 43, 101–118. https://doi.org/10.18172/cig.3131.

Pedersen, J., Hafner, S.D., 2023. Ammonia emissions after field application of anaerobically digested animal slurry: Literature review and perspectives. Agric. Ecosyst. Environ. 357, 108697. https://doi.org/10.1016/j.agee.2023.108697.

Pietsch, D., Kühn, P., 2017. Buried soils in the context of geoarchaeological research - two examples from Germany and Ethiopia. Archaeol. Anthropol. Sci. 9, 1571–1583. https://doi.org/10.1007/s12520-014-0180-9.

Pleasant, J.M.T., 2015. A new paradigm for pre-Columbian agriculture in North America. Early Am. Stud. 13, 374–412. http://www.jstor.org/stable/24474894.

Pötter, S., Schmitz, A., Lücke, A., Schulte, P., Obreht, I., Zech, M., Wissel, H., Marković, S. B., Lehmkuhl, F., 2021. Middle to Late Pleistocene environments based on stable organic carbon and nitrogen isotopes of loess-palaeosol sequences from the Carpathian Basin. Boreas 50, 184–204. https://doi.org/10.1111/bor.12470.

Quénard, L., Samouelian, A., Laroche, B., Cornu, S., 2011. Lessivage as a major process of soil formation: a revisitation of existing data. Geoderma 167 (168), 135–147. https://doi.org/10.1016/j.geoderma.2011.07.031.

Reimann, C., Garrett, R.G., 2005. Geochemical background—concept and reality. Sci. Total Environ. 350, 12–27. https://doi.org/10.1016/j.scitotenv.2005.01.047.

Reisser, M., Purves, R.S., Schmidt, M.W.I., Abiven, S., 2016. Pyrogenic carbon in soils: a literature-based inventory and a global estimation of its content in soil organic carbon and stocks. Front. Earth Sci. 4, 80. https://doi.org/10.3389/feart.2016.00080.

Rinklebe, J., Antoniadis, V., Shaheen, S.M., Rosche, O., Altermann, M., 2019. Health risk assessment of potentially toxic elements in soils along the Central Elbe River, Germany. Environ. Int. 126, 76–88. https://doi.org/10.1016/j.envint.2019.02.011.

Rogaar, H., Lothammer, H., van der Plas, L., Jongmans, A.G., Bor, J., 1993. Phaeozem and Luvisol development in relation to relief and climate in southwestern Rheinhessen, Germany. Mainz. Geowiss. Mitt. 22, 227–246.

Rumpel, C., Knicker, H., Kögel-Knabner, I., Hüttl, R.F., 1998. Airborne contamination of immature soil (Lusatian Mining District) by lignite-derived materials: its detection and contribution to the soil organic matter budget. Water Air Soil Pollut. 105, 481–492. https://doi.org/10.1023/A:1005080820520.

Schalich, J., 1988. Boden- und Landschaftsgeschichte. Rheinische Ausgrabungen 28, 17–29.

Schatz, T., 2023. Der Ackerboden als Archiv der Landnutzungsgeschichte. Rundbrief Grabungstechnik 22, 4–8.

Scherer, S., Höpfer, B., Deckers, K., Fischer, E., Fuchs, M., Kandeler, E., Lechterbeck, J., Lehndorff, E., Lomax, J., Marhan, S., Marinova, E., Meister, J., Poll, C., Rahimova, H., Rösch, M., Wroth, K., Zastrow, J., Knopf, T., Scholten, T., Kühn, P., 2021. Middle Bronze Age land use practices in the northwestern Alpine foreland – a multi-proxy study of colluvial deposits, archaeological features and peat bogs. Soil 7, 269–304. https://doi.org/10.5194/soil-7-269-2021.

Schlütz, F., Hofmann, R., Dal Corso, M., Pashkevych, G., Dreibrodt, S., Shatilo, M., Terna, A., Fuchs, K., Filipović, D., Flohr, P., Makarewicz, C.A., Țerna, S., Videiko, M., Rud, V., Müller, J., Kirleis, W., 2023. Isotopes prove advanced, integral crop production, and stockbreeding strategies nourished Trypillia mega-populations. Proc. Natl. Acad. Sci. 120, e2312962120. https://doi.org/10.1073/pnas.2312962120.

Schunke, T., 2018. Fahren oder Tragen? Methoden des Antransports von Baumaterial für bronzezeitliche Grabhügel. In: Nessel, B., Neumann, D., Bartelheim, M. (Eds.), Bronzezeitlicher Transport – Akteure, Mittel und Wege. RessourcenKulturen 8, Tübingen, pp. 85–115.

Schwahn, H.-J., Gahrmann, N., 1976. Der Mittlere Muschelkalk im östlichen Subherzyn. Hercynia N.F. 3, 332–339.

Semmel, A., 1995. Holozäne Bodenbildungsraten und "tolerierbare Bodenerosion" - Beispiele aus Hessen. Geol. Jahrb. 123, 125–131.

SLUG, 1992. Geologische Übersichtskarte des Freistaats Sachsen 1 : 400.000. Sächsisches Landesamt für Umwelt und Geologie, Freiberg.

SLULG, 1993. Bodenübersichtskarte Sachsen 1 : 400.000. Sächsisches Landesamt für Umwelt, Landwirtschaft und Geologie, Freiberg.

Šrámek, V., Slodičák, M., Lomský, B., Balcar, V., Kulhavý, J., Hadaš, P., Pulkráb, K., Šišák, L., Pěnička, L., Sloup, M., 2008. The ore mountains: will successive recovery of forests from lethal disease be successful? Mt. Res. Dev. 28, 216–221. https://doi.org/10.1659/mrd.1040.

Stika, H.-P., Heiss, A.G., 2014. Plant cultivation in the Bronze Age. In: Fokkens, H., Harding, A. (Eds.), The Oxford Handbook of the European Bronze Age. Oxford University Press, Oxford, UK, pp. 348–369.

Stoops, G., 2021. Guidelines for analysis and description of regolith thin sections, second ed. Wiley, Hoboken/NJ.

Storozum, M.J., Qin, Z., Wang, Y.V., Liu, H., 2020. Buried soils as archives of paleo-pollution in the North China Plain. Anthropocene 31, 100251. https://doi.org/10.1016/j.ancene.2020.100251.

Thevenot, M., Dignac, M.-F., Rumpel, C., 2010. Fate of lignins in soils: a review. Soil Biol. Biochem. 42, 1200–1211. https://doi.org/10.1016/j.soilbio.2010.03.017.

Thies, J.E., Grossman, J.M., 2023. The soil habitat and soil ecology. In: Uphoff, N., Thies, J. (Eds.), Biological approaches to regenerative soil systems. CRC Press, Boca Raton, pp. 59–78.

Tian, D., Niu, S., 2015. A global analysis of soil acidification caused by nitrogen addition. Environ. Res. Lett. 10, 024019. https://doi.org/10.1088/1748-9326/10/2/024019.

Tinapp, C., Stäuble, H., 2000. Auenentwicklung und Besiedlungsgeschichte im Tal der Weißen Elster südlich von Leipzig. Trierer Geographische Studien 23, 31–48.

Tinapp, C., Gumnior, M., Heinrich, S., Herbig, C., Kretschmer, S., Schneider, B., Stäuble, H., Stobbe, A., 2025. Holocene vegetation dynamics and sedimentation processes in a small depression on a Pleistocene plain – a multi-proxy approach for the palaeoenvironmental reconstruction of a Neolithic settlement area near Leipzig, Saxony. E & G - Quaternary Sci. J. 74, 79–99. https://doi.org/10.5194/egqsj-74-79-2025.

von Suchodoletz, H., Tinapp, C., Lauer, T., Glaser, B., Stäuble, H., Kühn, P., Zielhofer, C., 2019. Distribution of chernozems and phaeozems in Central Germany during the Neolithic period. Quat. Int. 511, 166–184. https://doi.org/10.1016/j.quaint.2017.10.041.

von Suchodoletz, H., van Meer, M., Kühn, P., Wiedner, K., Schunke, T., Reimann, T., 2023. Deciphering timing and rates of central German Chernozem/Phaeozem formation through high resolution single-grain luminescence dating. Sci. Rep. 13, 4769. https://doi.org/10.1038/s41598-023-32005-9.

von Suchodoletz, H., Khosravichenar, A., Fütterer, P., Zielhofer, C., Schneider, B., Sprafke, T., Tinapp, C., Fülling, A., Werther, L., Stäuble, H., Veit, U., Ettel, P., Werban, U., Miera, J., 2024. Holocene overbank sedimentation in Central Europe between natural and human drivers - the Weiße Elster River (Central Germany). Geomorphology 449, 109067. https://doi.org/10.1016/j.geomorph.2024.109067.

von Suchodoletz, H., Schneider, B., Skokan, A., Nitz, T., Glaser, B., Polivka, S., Wiedner, K., Schlütz, F., Schunke, T., Kühn, P. (in press): Analytical data of a buried and a recent surficial Chernozem in the Bornhöck area in Central Germany. PANGAEA. https://doi.pangaea.de/10.1594/PANGAEA.982395.

Wagenbreth, O., Steiner, W., 1989. Geologische Streifzüge. VEB Deutscher Verlag für Grundstoffindustrie, Leipzig.

Wang, T.-H., Wang, Q.-B., Han, C.-L., Cui, D., Sauer, D., 2023. Development and application of new transfer functions between climate and soil weathering indices for paleoclimatic reconstructions from Chinese loess-paleosol sections. Catena 224, 106974. https://doi.org/10.1016/j.catena.2023.106974.

Wennrich, V., Wagner, B., Melles, M., Morgenstern, P., 2005. Late glacial and Holocene history of former Salziger See, Central Germany, and its climatic and environmental implications. Int. J. Earth Sci. 94, 275–284. https://doi.org/10.1007/s00531-005-0468-1.

Wetstone, G., Foster, S., 1983. Acid precipitation: what is it doing to our forests? Environ. 25, 10–40. https://doi.org/10.1080/00139157.1983.9940939.

Wisniewski, A., Plonka, T., Jary, Z., Lisa, L., Traczyk, A., Kufel-Diadowska, B., Raczyk, J., Bajer, A., 2015. The early Gravettian in a marginal area: New evidence from SW Poland. Quat. Int. 359 (360), 131–152. https://doi.org/10.1016/j.quaint.2014.10.003.

Wisniewski, A., Jary, Z., Moska, P., Pyzewicz, K., Ciombor, M., Krawczyk, M., Kasprzak, M., 2022. Middle Palaeolithic, transitional or upper Palaeolithic:

geoarchaeological revision of the southern part of the loess site Dzierzysław 1, SW Poland. Quat. Int. 632, 94–111. https://doi.org/10.1016/j.quaint.2021.10.015.

Zapolska, A., Serge, M.A., Mazier, F., Quiquet, A., Renssen, H., Vrac, M., Fyfe, R., Roche, D.M., 2023. More than agriculture: analysing time-cumulative human impact on European land-cover of second half of the Holocene. Quat. Sci. Rev. 314, 108227. https://doi.org/10.1016/j.quascirev.2023.108227.

Zikeli, S., Jahn, R., Kastler, M., 2002. Initial soil development in lignite ash landfills and settling ponds in Saxony-Anhalt, Germany. J. Plant Nutr. Soil Sci. 165, 530–536. https://doi.org/10.1002/1522-2624(200208)165:4<530::AID-JPLN530>3.0.CO;2-J.

Zink, M., Kumar, R., Cuntz, M., Samaniego, L., 2017. A high-resolution dataset of water fluxes and states for Germany accounting for parametric uncertainty. Hydrol. Earth Syst. Sci. 21, 1769–1790. https://doi.org/10.5194/hess-21-1769-2017.